1 **Revisiting the Relationship between Atlantic Dust and Tropical Cyclone**
2 **Activity using Aerosol Optical Depth Reanalyses: 2003-2018**
3
4 Peng Xian[1a], Philip J. Klotzbach[2a], Jason P. Dunion[3], Matthew A. Janiga[1], Jeffrey S. Reid[1] , Peter
5 R. Colarco[4] and Zak Kipling[5]
6
7 [1]Naval Research Laboratory, Monterey, CA, USA.
8 [2]Department of Atmospheric Science, Colorado State University, Fort Collins, CO, USA.
9 [3]University of Miami/RSMAS/CIMAS – NOAA/AOML/Hurricane Research Division, Miami,
10 FL, USA.
11 [4]NASA Goddard Space Flight Center, Greenbelt, MD, USA.
12 [5]European Centre for Medium-Range Weather Forecasts, Reading, UK.
13
14 [a] Peng Xian and Philip J. Klotzbach are joint-lead coauthors.
15 Correspondence: Peng Xian (peng.xian@nrlmry.navy.mil)
16
17
18

19

20

21

22

23

24

25

26

27

28

29

30

31

32

33

34

Abstract

Previous studies have noted a relationship between African dust and Atlantic tropical cyclone (TC) activity. However, due to the limitations of past dust analyses, the strength of this relationship remains uncertain. The emergence of aerosol reanalyses, including the Navy Aerosol Analysis and Prediction System (NAAPS) Aerosol Optical Depth (AOD) reanalysis, NASA Modern-Era Retrospective analysis for Research and Applications, Version-2 (MERRA-2) and ECMWF Copernicus Atmosphere Monitoring Service reanalysis (CAMSRA) enable an investigation of the relationship between African dust and TC activity over the tropical Atlantic and Caribbean in a consistent temporal and spatial manner for 2003-2018. Although June-July-August (JJA) 550 nm dust AOD (DAOD) from all three reanalysis products correlate significantly over the tropical Atlantic and Caribbean, the difference in DAOD magnitude between products can be as large as 60% over the Caribbean and 20% over the tropical North Atlantic. Based on the three individual reanalyses, we have created an aerosol multi-reanalysis-consensus (MRC). The MRC presents overall better root mean square error over the tropical Atlantic and Caribbean compared to individual reanalyses when verified with ground-based AErosol RObotic NETwork (AERONET) AOD measurements. Each of the three individual reanalyses and the MRC have significant negative correlations between JJA Caribbean DAOD and seasonal Atlantic Accumulated Cyclone Energy (ACE), while the correlation between JJA tropical North Atlantic DAOD and seasonal ACE is weaker. Possible reasons for this regional difference are provided. A composite analysis of three high versus three low JJA Caribbean DAOD years reveals large differences in overall Atlantic TC activity. We also show that JJA Caribbean DAOD is significantly correlated with large-scale fields associated with variability in interannual Atlantic TC activity including zonal wind shear, mid-level moisture and SST, as well as ENSO and the Atlantic Meridional Mode (AMM), implying confounding effects of these factors on the dust-TC relationship. We find that seasonal Atlantic DAOD and the AMM, the leading mode of coupled Atlantic variability, are inversely related and intertwined in the dust-TC relationship.

1. Introduction

Saharan dust particles can affect weather and climate through both direct and indirect radiative and cloud processes, notably in association with boreal summer Saharan Air Layer (SAL) outbreaks. The SAL is a layer of hot and dry air that forms over continental West Africa and is then advected over the low-level moist marine boundary layer of the tropical Atlantic (Carlson & Prospero, 1972). The SAL is often associated with the African Easterly Jet (AEJ) that can enhance vertical wind shear. Despite numerous observational and modeling studies that have examined the relationships between these aspects of the SAL and Atlantic TC activity, there are conflicting findings as to whether dust acts to generally inhibit or enhance tropical cyclogenesis and intensification. Some studies suggest negative impacts of the SAL's dust-laden dry air and the AEJ on TC activity (e.g., Dunion and Velden 2004; Lau and Kim 2007; Jones et al. 2007; Sun et al. 2008; Pratt and Evans 2008) while others have focused exclusively on the dust particles themselves and have found a negative influence on TCs (e.g., Evan et al. 2006a; Rosenfield et al. 2007; Strong et al. 2018; Reed et al. 2019). Other studies have suggested little impact of the SAL on TCs (e.g., Braun 2010; Sippel et al. 2011; Braun et al. 2013), while others have posited a positive impact of dust on TCs through cloud-microphysical processes (e.g., Jenkins et al. 2008). Finally, others have suggested that there are contrasting influences through different mechanisms and for different TCs (Karyampudi and Pierce, 2002; Bretl et al. 2015; Pan et al., 2018), highlighting the complexity of the dust-TC interaction.

African dust impacts the North Atlantic throughout the year, with its summer peak season (May-August) overlapping and leading the peak of the Atlantic hurricane season (August-October; Figure S1). As African dust outbreaks during the summer are often associated with the SAL, airborne dust has often been used as an indicator for the SAL (Dunion & Velden, 2004; Dunion, 2011; Tsamalis et al., 2013), although early season cases where the majority of the dust existed in the marine boundary layer below the trade wind inversion instead of staying aloft were also found (Reid et al., 2003). Saharan dust and the SAL are frequently observed throughout the Caribbean and as far west as Central America and the North American continent during the boreal summer (e.g., Prospero, 1999; Reid et al., 2003; Dunion & Velden 2004; Nowottnick et al., 2011; Kuciauskas et al., 2018). Airborne dust associated with the SAL often extends to 5.5 km (500 hPa) off of western Africa, and becomes thinner as its top lowers and its base rises as it is advected westward, shrinking to below 2 km in the Caribbean and in the Gulf of Mexico (Tsamalis et al., 2013). In some strong SAL cases, however, the top of the dust layer can reach 6 km (Reid et al., 2003; Colarco et al., 2003). During their trans-Atlantic transport, dust aerosols are from time to time observed to interact with TCs, as seen in satellite imagery (Figure 1).

African dust and its associated SAL has been hypothesized to impact TCs through a variety of mechanisms. Through scattering and absorbing sunlight, dust reduces solar radiation reaching the surface, thus cooling SSTs (e.g., Miller and Tegen, 1998; Lau and Kim 2007; Evan et al., 2009). Lower SSTs provide TCs with less energy to initiate, develop, and maintain strength. Through additional radiative heating of the dusty layer, mineral dust is also suggested to impact the structure, location and energetics of the AEJ (Tompkins et al., 2005; Wilcox et al., 2010; Reale et al., 2011) and African easterly wave (AEW) activity (Karyampudi and Carlson, 1988; Reale et al., 2009; Nathan et al., 2017; Jones et al., 2004; Ma et al., 2012; Grogan et al., 2016, 2017; Bercos-Hickey et al., 2017), thus having implications for tropical cyclogenesis. From a thermodynamic point of view, Dunion and Velden (2004) have proposed that the dust-carrying

3

107 SAL outbreaks could inhibit TC formation and development in the North Atlantic through three
108 primary mechanisms, including dry air intrusion into the storm, enhancement of the local vertical
109 wind shear associated with the enhanced AEJ, and stabilization of the environment due to
110 radiative heating of the dust layer above the marine boundary layer.

111 Dust particles can also act as cloud condensation nuclei (Twohy et al., 2009; Karydis et al.,
112 2011) and ice nuclei (DeMott et al., 2003; Sassen et al., 2003) and affect cloud microphysics,
113 weakening or strengthening convection depending on the environment (Khain, 2009). Focusing
114 specifically on TCs, there is not a consistent conclusion among studies on whether the
115 microphysical impacts of dust weaken or strengthen TCs (Jenkins et al., 2008; Rosenfeld et al.,
116 2007; Zhang et al., 2007, 2009; Herbener et al., 2014; Nowottnick et al., 2018).

117 While dust aerosols can affect TC formation and development through radiative and cloud-
118 microphysical impacts, TCs can in turn impact dust aerosol spatial distributions through wet
119 removal and dynamic flow (Herbener et al., 2016). AEWs, serving as seeding disturbances for
120 TCs (Landsea, 1993), are shown to contribute to dust emission and transport (e.g., Westphal et
121 al., 1987; Jones et al., 2003; Knippertz and Todd, 2010). Climate variability that affects TC
122 activity can also impact African dust emission and transport over the North Atlantic and
123 Caribbean. For example, ENSO was found to affect the emission and transport of African dust as
124 well (Prospero & Lamb, 2003; DeFlorio et al., 2016), especially during the boreal winter
125 (Prospero & Nees, 1986; Evan et al., 2006b).

126 How all of these factors interact in the complex climate system and to what extent they can
127 impact TC formation and intensification is still largely unknown. The goal of this study is to
128 explore how the integrated interactions manifest themselves in the relationship between Saharan
129 dust and Atlantic TC activity on seasonal to interannual time scales using state-of-the-art aerosol
130 reanalysis data. This serves as a first step towards further understanding the dust-TC relationship
131 and evaluating the relative importance of different mechanisms. Previous empirical studies on
132 the relationship between African dust and Atlantic TC activity are limited by uneven spatial and
133 temporal sampling by satellite and in situ-based observations. The emergence of several aerosol
134 reanalysis datasets, including the Navy Aerosol Analysis and Prediction System (NAAPS)
135 Aerosol Optical Depth (AOD) reanalysis (NAAPS-RA, Lynch et al., 2016), the Modern-Era
136 Retrospective analysis for Research and Applications, Version 2 (MERRA-2) aerosol reanalysis
137 (Randles et al., 2017) and the Copernicus Atmosphere Monitoring Service ReAnalysis
138 (CAMSRA) (Inness et al., 2019) allow us to investigate this relationship in a more consistent
139 manner over their joint time period to provide a degree of statistical robustness.

140 In section 2, an introduction to the aerosol and large-scale environmental data and the analysis
141 methods employed is provided. Section 3 presents the DAOD climatology, its interannual
142 variability over the Atlantic, and comparisons of the three aerosol reanalyses. This section also
143 evaluates correlations between DAOD and Atlantic TC activity, as well as the relationship
144 between DAOD and large-scale environmental conditions and climate modes. The sensitivity of
145 the results to the definition of the regions, the number of composite years used, and the definition
146 of dust seasons are provided in section 4. A discussion and conclusions are given in section 5.

147 **2. Data and Methods**

148 **2.1 Methods**

149 Regardless of the underlying mechanisms, as there are contradicting mechanisms proposed in
150 different studies, the goal of this study is to examine if there is a robust and statistically
151 significant relationship between African dust and Atlantic TC activity on seasonal to interannual
152 time scales. We also examine if there are confounding factors, for example, meteorological
153 conditions and climate modes that co-vary with dust and hence influence TC activity.

154 We use dust AOD (DAOD) to represent Atlantic dust levels. Three aerosol reanalysis products,
155 and their consensus DAOD are used in order to increase the fidelity of the analysis result, given
156 that multi-model-consensus typically has been shown to have better data quality in prior
157 assessments (Sessions et al., 2015; Xian et al., 2019). Various TC count indices and
158 Accumulated Cyclone Energy (ACE) (Bell et al. 2000), defined in the next section, are utilized
159 to represent TC activity.

160 The Atlantic Main Development Region (MDR) (e.g., Goldenberg et al., 2001), including the
161 Caribbean (10-20°N, 85-60°W) and the tropical North Atlantic (10-20°N, 60-20°W), are the
162 focus regions for this study (see also Figure 2 for a spatial representation of the two subregions).
163 Most previous studies of dust impacts on TC activity have focused on the tropical North Atlantic
164 or regions closer to the African continent (e.g., Karyampudi and Pierce, 2002; Bretl et al. 2015;
165 Pan et al., 2018) where DAOD is relatively high. However significant dust pulses can also be
166 transported into the Caribbean. We therefore expand our study area to explore the potential
167 impacts of high levels of dust in the Caribbean on Atlantic TC activity. This allows us to explore
168 regional differences in the dust-TC relationship. Statistical relationships between DAOD and TC
169 activity over the MDR are investigated using the three aerosol reanalyses and multi-reanalysis-
170 consensus (MRC). The results obtained herein also help us assess the potential of using DAOD
171 to aid in future Atlantic seasonal hurricane forecasts.

172 The correlations between variables of interest are based on the Pearson correlation coefficient.
173 Statistical significance is assessed at the 95% level using a two-tailed Student's t-test.
174 Correlations >= 0.51 are statistically significant given that a 16-year time period (e.g., 2003-
175 2018) is investigated here. For partial correlation analysis, partial correlations >=0.55 are
176 statistically significant at the 95% level with 13 degrees of freedom. The criteria for statistical
177 significance with various degrees of freedom can also be obtained at:
178 https://www.esrl.noaa.gov/psd/data/correlation/significance.html.

2.2 Aerosol data

180 A combination of aerosol reanalyses are used to describe the aerosol environment over the
181 tropical North Atlantic and Caribbean. An aerosol multi-reanalysis-consensus (MRC) based on
182 three aerosol reanalysis products, including the NAAPS-RA (Lynch et al., 2016) from the US
183 Naval Research Laboratory, MERRA-2 (Randles et al., 2017) from NASA, and CAMSRA
184 (Inness et al., 2019) from ECMWF, are also generated and used. The analysis period is focused
185 on 2003-2018, when all three aerosol reanalyses are available and both Terra and Aqua Moderate
186 Resolution Imaging Spectroradiometer (MODIS) AOD retrievals were assimilated therein.

2.2.1 NAAPS AOD reanalysis

188 The NAAPS-RA product provides 550 nm speciated AOD at a global scale with 1°x1° degree
189 spatial and 6-hourly temporal resolution for the years 2003-2018 (Lynch et al., 2016). This

190 reanalysis uses a modified version of NAAPS and assimilates quality-controlled AOD retrievals
191 from MODIS on Terra and Aqua and the Multi-angle Imaging SpectroRadiometer (MISR) on
192 Terra (Zhang et al., 2006; Hyer et al., 2011; Shi et al., 2011). NAAPS characterizes
193 anthropogenic and biogenic fine aerosol species (ABF), dust, sea salt and biomass burning
194 smoke aerosols. The aerosol source functions were tuned regionally so that a best match between
195 the model coarse and fine mode AODs and the Aerosol Robotic Network (AERONET) AODs
196 can be obtained. Other model processes, e.g. deposition, were also tuned to minimize the AOD
197 difference between the model and quality-controlled satellite AOD retrievals. NOAA Climate
198 Prediction Center MORPHing (CMORPH) precipitation derived from satellite observations
199 (Joyce et al., 2004) is used to correct precipitation biases in the tropics for better AOD analyses
200 through wet deposition processes (Xian et al., 2009). The reanalysis captures the decadal AOD
201 trends detected using standalone satellite products in other studies (e.g., Hsu et al., 2012; Zhang
202 et al., 2017), demonstrating the quality of the reanalysis product for climate studies. The
203 NAAPS-RA data for May 2017 - November 2018 was generated by assimilating MODIS DA-
204 quality AOD only without MISR AOD assimilation because of the unavailability of MISR DA-
205 quality data at the time of this study. The impact of not including MISR is expected to be minor
206 as MISR provides only about 10% of the total assimilated AOD data. Additionally, differences
207 between monthly mean DA-quality AOD over the MDR region derived using both MODIS and
208 MISR versus using only MODIS were found to be negligible (not shown).

2.2.2 MERRA-2 AOD reanalysis

210 As part of the upgrade from the original MERRA reanalysis (Rienecker et al., 2011) based on the
211 Goddard Earth Observing System (GEOS) Earth system model, MERRA-2 now incorporates
212 assimilation of AOD from a variety of remote sensing sources, including AERONET, MODIS,
213 and MISR after 2000, and AVHRR before 2002. The aerosol module used for MERRA-2 is the
214 Goddard Chemistry, Aerosol, Radiation, and Transport model (GOCART; Chin et al. 2000;
215 Colarco et al., 2010), which provides simulations of dust, sea salt, black and organic carbon, and
216 sulfate aerosols, and is run radiatively coupled to the GEOS AGCM. A detailed description and
217 validation of the AOD reanalysis product can be found in Randles et al. (2017) and Buchard et
218 al. (2017). For the purpose of this study, monthly mean DAOD at 550 nm with 0.5° latitude and
219 0.625° longitude spatial resolution is used. MERRA-2's longer data record (1981-present)
220 would have made it an ideal candidate for a longer-period analysis of the relationship between
221 DAOD and TCs. However, the volcanic eruptions of El Chichon (1982) and Pinatubo (1991)
222 result in high AOD for several years following each event, and the particle property assumptions
223 in MERRA-2 do not properly apportion the assimilated AOD increments among the simulated
224 aerosol species. For the 2003-2018 time period, MERRA-2 AOD data has similar validation
225 statistics compared to NAAPS-RA and CAMSRA at the sites located off of the coast of West
226 Africa and the Caribbean, as shown in Table 1.

2.2.3 CAMSRA AOD reanalysis

228 Under the banner of the Copernicus Atmosphere Monitoring Service (CAMS), operated by
229 ECMWF on behalf of the European Commission, a new global reanalysis of atmospheric
230 composition has been produced: CAMSRA (Inness et al., 2019). This is the successor to the
231 MACC reanalysis (Inness et al., 2013) and CAMS interim reanalysis (Flemming et al., 2017)
232 produced previously at ECMWF. The dataset spans the period 2003–2018 and is being continued
233 for subsequent years. The model component is based on the same Integrated Forecasting System

234 (IFS) used at ECMWF for weather forecasting and meteorological reanalysis, but at a coarser
235 resolution and with additional modules activated for prognostic aerosol species (dust, sea salt,
236 organic matter, black carbon and sulphate) and trace gases. The impact of the aerosols (and
237 ozone) on radiation and thereby on meteorology is included in the model. For aerosol,
238 observations of total AOD at 550nm are assimilated from MODIS (Terra and Aqua) for the
239 whole period, and from the Advanced Along-Track Scanning Radiometer for 2003–2012, using a
240 4D variational data assimilation system with a 12-hour data assimilation window along with
241 meteorological and trace gas observations. The speciated AOD products used in this study are
242 available at a 3-hourly temporal resolution and a ~0.7° spatial resolution. Model development
243 has generally improved the speciation of aerosols compared with earlier reanalyses, and
244 evaluation against AERONET is largely consistent over the period of the reanalysis. There is a
245 known issue regarding a significant overestimation of sulfate near outgassing volcanoes;
246 however this is unlikely to have much relevance to the regions considered in this study.

247 **2.2.4 AOD multi-reanalysis-consensus (MRC)**

248 Based on the three aerosol reanalysis products described above, we made a MRC product
249 following the multi-model-ensemble method of the International Cooperative for Aerosol
250 Prediction (ICAP, Sessions et al., 2015; Xian et al., 2019). The MRC is a consensus mean of the
251 three individual reanalyses, with a 1°x1° degree spatial and monthly temporal resolution.
252 Speciated AODs and total AOD at 550nm for 2003-2018 are available. This new product is
253 validated with ground-based AERONET observations for African-dust-influenced regions,
254 including the western coast of North Africa and the Caribbean Sea. Validation results in terms of
255 RMSE for total and coarse-mode AODs are presented in Table 1. Similar to the ICAP multi-
256 model-ensemble evaluation result, the MRC is found to generally be the top performer among all
257 of the reanalyses for the study region.

258 **2.2.5 AErosol RObotic NETwork (AERONET) fine and coarse mode AOD**

259 AERONET is a ground-based global scale sun photometer network that includes instruments to
260 measure sun and sky radiance at wavelengths ranging from the near ultraviolet to the near
261 infrared during daytime hours. This network has been providing high-accuracy and high-quality
262 measurements of aerosol properties since the 1990s (Holben et al., 1998; Holben et al., 2001)
263 and is often used as the primary dataset for validating aerosol optical properties in satellite
264 retrievals and model simulations (e.g., Levy et al., 2010; Colarco et al., 2010; Kahn & Gaitley,
265 2015). Only cloud-screened, quality-assured version 3 Level 2 AERONET data are utilized in
266 this study (Giles et al., 2019). AERONET multiple wavelength measurements were used to
267 derive both fine and coarse mode AODs at 550 nm based on the Spectral Deconvolution Method
268 (SDA) of O'Neill et al. (2003). The SDA product was verified with in situ measurements (Kaku
269 et al., 2014) and was shown to be able to capture the full modal properties of fine and coarse
270 particles. Temporally, AERONET data are averaged into 6-hr bins centered at the regular model
271 output times of 0, 6, 12 and 18 UTC. Monthly mean AERONET AOD is derived only when the
272 total number of 6-hr AERONET data is greater than 18 to ensure temporal representativeness.

273 **2.3 Tropical Cyclone data – HURDAT2**

274 Atlantic basin TC data were taken from the Atlantic hurricane database version 2 (HURDAT2;
275 Landsea & Franklin, 2013). This dataset contains six-hourly information (including position,

276 maximum sustained winds, and central pressure – where available) for every TC observed in the
277 Atlantic basin dating back to 1851.

278 **2.4 Atmospheric data - ERA-Interim Reanalysis**

279 The ERA-Interim Reanalysis (Dee et al., 2011) is a global atmospheric reanalysis produced by
280 the ECMWF that uses a 4-dimensional variational analysis with a 12-hour analysis window. The
281 spectral resolution of this data is approximately 80 km (T255) and is available on 60 vertical
282 levels from the surface to 0.1 hPa and is available from January 1979 – August 2019. We use
283 monthly mean large-scale fields, including vector wind, atmospheric temperature and relative
284 humidity data on several pressure levels.

285 **2.5 Oceanic data - NOAA OI SST**

286 The National Oceanic and Atmospheric Administration (NOAA) Optimum Interpolation (OI)
287 SST product (Reynolds et al., 2002) is utilized for SST calculations. NOAA OI SST v2 uses a
288 combination of in-situ data, satellite data, SSTs simulated by sea-ice cover, and bias adjustments
289 to arrive at its final estimate of SSTs. NOAA OI SST V2 data is available on a 1° x 1° grid from
290 November 1981-present.

291 **2.6 Climate indices**

292 The Oceanic Nino Index (ONI), defined to be a three-month average of the Niño 3.4 (5°S-5°N,
293 170-120°W) index (Barnston et al., 1997) based on centered 30-year periods which are updated
294 every five years, is utilized to represent the state of El Niño-Southern Oscillation (ENSO). This
295 index is also used by NOAA to identify ENSO events.

296 The SST component of the AMM (Kossin & Vimont, 2007) is investigated to assess the
297 relationship between DAOD and tropical Atlantic oceanic conditions. While the index is not
298 standardized, we have standardized it by its 1981-2010 average and standard deviation.

299 **2.7 Derived tropical cyclone indices**

300 The genesis potential index (GPI) was calculated using monthly-averaged ERA-Interim data
301 following Emanuel and Nolan (2004). The maximum potential intensity (MPI) was calculated
302 using monthly-averaged ERA-Interim temperature and moisture and NOAA OI SST following
303 Bister and Emanuel (2002).

304 **3. Results**

305 **3.1 Dust aerosol optical depth over the MDR (2003-2018)**

306 Figure 2 shows the MRC monthly DAOD climatology based on the 2003-2018 average as well
307 as the ratio of DAOD to total AOD for June-October over the tropical Atlantic. Climatologically
308 from June-October, the majority of airborne dust originates from the Sahara Desert, in contrast to
309 the winter season when a significant amount of dust is emitted over the Sahel and southern
310 Sahara (Engelstaedter & Washington, 2007). This dust is then transported westward over the
311 Atlantic and eventually to the Caribbean, largely within the 10-25°N latitude belt. The
312 transported African dust covers most of the Atlantic hurricane MDR, which spans the tropical
313 North Atlantic and Caribbean. The DAOD over the Atlantic is, on average, much higher in June,

314   July, and August (JJA) than in September and October because of higher emissions over the
315   African continent in the former months (Carlson and Prospero 1972; Engelstaedter and
316   Washington, 2007; Dunion & Marron, 2008; Dunion, 2011). DAOD is also much higher over the
317   tropical Atlantic than over the Caribbean, as dust aerosols are removed by wet and dry processes
318   during the long-range transport. The MRC shows that dust aerosols are the dominant contributor
319   to the total AOD in the MDR during most of the hurricane season (June-October). The DAOD
320   accounts for about 50-60% of the total AOD over the tropical North Atlantic and around 30-50%
321   over the Caribbean for JJA. This suggests that the total AOD can be a relatively good indicator
322   of DAOD in the tropical North Atlantic but is not as good of an indicator in the Caribbean for
323   JJA. The DAOD contribution to total AOD is about 10-20% less for September and October.
324   Considering the potential larger forcing by airborne dust in JJA than in September and October,
325   the focus season in this study is JJA.

326   As transport of Saharan dust across the Atlantic during summer is often associated with SAL
327   outbreaks, which are approximately centered around 700 hPa (Dunion & Velden, 2004; Dunion,
328   2011), monthly climatological 700 hPa relative humidity (RH) and horizontal wind are also
329   shown in Figure 2. Climatologically, the MDR is dominated by the mid-level easterly jet (7-8 m
330   s^{-1}) during JJA and weaker easterlies (5-6 m s^{-1}) during September and October. Over the
331   Caribbean, the wind direction veers slightly towards the north for all of the studied months and
332   relates to this region being typically positioned on the west side of the climatological Atlantic
333   subtropical ridge. 700 hPa RH is on the order of 40% and 50% for the tropical Atlantic and the
334   Caribbean respectively for JJA and is about 10% higher in September and October. RH is higher
335   in the Caribbean than in the tropical North Atlantic as the impact of dry air from the SAL and
336   from upper-level subsidence becomes weaker from east to west. For context, the Atlantic moist
337   tropical sounding, defined in Dunion (2011), has average 700 hPa winds of 3.6 m s^{-1} at 112°
338   (wind direction) and 66% RH, while the mean SAL sounding has corresponding values of 7.8 m
339   s^{-1} at 91° and 34% RH.

340   Figure 3 shows the monthly mean AERONET version 3 L2 and MRC 550 nm modal AOD time
341   series at four AERONET sites that are primarily influenced by African dust. From east to west,
342   these sites include Dakar, Senegal (14.4°N, 17.0°W), Cape Verde (16.7°N, 22.9°W), Ragged
343   Point, Barbados (13.2°N, 59.4°W), and La Parguera, Puerto Rico (18.0°N, 67.0°W), which are
344   also marked in Figure 1. The boreal summer peak dust activity (i.e., JJA) is highlighted. Dust
345   aerosols are typically considered coarse-mode, although there may be a very small amount of
346   mass in fine-mode. The fine-mode AOD observed in AERONET measurements for these sites
347   are normally dominated by pollution and biomass-burning smoke. Dakar and Cape Verde
348   experience dust aerosols throughout the year, with a peak in JJA and a weaker secondary peak
349   during the boreal winter, which is associated with dust emissions from the Sahel. The Ragged
350   Point and La Parguera sites, which are remote receptor sites in the Caribbean, are influenced by
351   African dust predominantly during boreal summer, thus displaying a pronounced peak of total
352   and coarse-mode AODs in JJA. The secondary AOD peak during winter at Dakar and Cape
353   Verde is generally not observed at Ragged Point or La Parguera, as African dust is transported to
354   the south following the low-to-mid-level trade wind flow, occasionally reaching South America
355   (Prospero, 2014).

356   Figure 3 also shows the bias, the root mean square error (RMSE) of MRC and the correlation (*r*)
357   between MRC and AERONET for monthly AODs at each of the four AERONET sites. Overall,

9

MRC follows the seasonal and interannual variability in AERONET data for the total AOD quite well, and to a slightly lesser extent for the coarse-mode AOD. Coarse-mode aerosols include dust and sea salt, but are dominated by dust aerosols over the tropical North Atlantic for JJA (Figure 2c, speciated AOD cannot be obtained from AERONET measurements). The correlation is >~0.9 for the coarse-mode AOD and tends to be better at the long-range transport sites (i.e., Ragged Point and La Parguera) than the sites close to the dust source (i.e., Dakar and Cape Verde). The correlation is slightly lower in the source area than in the long-range transport region because there are large uncertainties in emissions and strong gradients due to local aerosol sources in the source area. Also, the source area allows less time for AOD data assimilation to correct aerosol mass loads, in addition to a lower signal/noise ratio of AOD retrievals over land than over water (e.g., Levy et al., 2005). The small bias, low RMSE and the high correlation with AERONET data illustrate the ability of MRC to capture the aerosol environment in the MDR. In addition, all of the three individual aerosol reanalyses that form the foundation of MRC have similar verification scores against AERONET, though the MRC typically has a better verification score than the individual reanalyses (Table 1). If we were to give different qualitative ratings for the three individual reanalyses for the study area, MERRA-2 is slightly better over North Africa and NAAPS-RA is slightly better over the Caribbean in terms of coarse-mode and total AOD RMSEs.

Figure 4 shows the time series of monthly mean and regionally-averaged DAOD from MRC and the three contributing reanalyses from 2003-2018 for the tropical North Atlantic and Caribbean as defined in Fig. 2. The DAODs from the three reanalyses have similar seasonal and interannual variability and are highly correlated, with $r >= 0.95$ for the entire 16-yr period and $r >= 0.85$ for JJA for both regions based on monthly means. The magnitudes of JJA DAOD from the three individual reanalyses are comparable over the tropical North Atlantic, with a 20% maximum difference among the three products based on JJA DAOD. The climatological average of JJA DAOD over the tropical North Atlantic is 0.21. The difference can be as much as ~0.06 (a ~60% difference between member products) for the Caribbean. The climatological average of JJA DAOD in the Caribbean is 0.10. Since the total and coarse-mode AOD verification statistics for the three products at the Caribbean AERONET sites are similar (Table 1), the DAOD difference is most likely due to the different partitioning of aerosol species (e.g., dust versus sea salt aerosols) during the total AOD data assimilation process. This is related to the fact that total AOD is the only aerosol property constrained by satellite observations through AOD data assimilation in all three aerosol reanalysis products, while speciated AOD is not constrained (Lynch et al., 2016; Randles et al., 2017; Inness et al., 2019). Nevertheless, the DAOD from the MRC is likely the most reliable given the generally better performance of multi-aerosol model consensus compared to individual aerosol models (Sessions et al., 2015; Xian et al., 2019).

3.2 Relationship between North Atlantic TC activity and JJA DAOD

Accumulated Cyclone Energy (ACE) is often utilized to represent TC activity and is defined to be the square of the one-minute maximum sustained wind speed at each six-hourly interval when a tropical or subtropical cyclone (with maximum sustained winds >=34 kt) is present (Bell et al., 2000). Basin-wide ACE is used here, as it is assumed that MDR conditions affect to some extent, the ACE of all storms that pass through the MDR, including those that later moved out of the MDR. For example, we hypothesize that in an active dust year, the suppressed conditions in the MDR would make for weaker, less organized AEWs that have less of a chance for formation

402   even if they do eventually move out of the MDR. Later we show in Table 2 that using ACE
403   generated in the Caribbean domain yields a consistent (same sign) yet stronger correlation
404   relationship between DAOD and ACE.

405   Atlantic TC activity shows a statistically significant relationship with regionally-averaged
406   Caribbean JJA DAOD. Figure 5a displays this relationship, with higher Caribbean DAOD
407   correlating ($r = -0.61$ with MRC DAOD and r of similar magnitudes from all three individual
408   reanalyses and exceeding the two-tailed 95% statistical significance level) with quieter Atlantic
409   hurricane seasons as quantified by ACE. While tropical North Atlantic DAOD and Caribbean
410   DAOD in JJA correlate strongly ($r = 0.88$), Figure 5b shows that the relationship between
411   DAOD and ACE is weaker in the tropical North Atlantic than in the Caribbean. The correlation
412   between tropical North Atlantic DAOD and ACE is -0.41, which falls below the statistical
413   significance threshold (correlations with MERRA-2 and CAMSRA DAODs are also
414   insignificant). We will show in the next section that the relationship between large-scale fields
415   known to impact Atlantic TC activity also tend to have higher correlations with JJA Caribbean
416   DAOD than with JJA tropical North Atlantic DAOD.

417   Given the strength of the relationship between Caribbean DAOD and seasonal Atlantic ACE, we
418   next investigate the relationship in extreme JJA DAOD seasons. We take the three seasons from
419   2003-2018 when JJA Caribbean DAOD was at its highest levels and when it was at its lowest
420   levels.

421   The three seasons with the highest JJA Caribbean DAOD were 2018, 2015 and 2014 in
422   descending order, and the three seasons with the lowest JJA Caribbean DAOD were 2005, 2011
423   and 2017 in ascending order based on MRC. The left column of Figure 6 shows DAOD
424   composites for the three high and the three low JJA Caribbean DAOD seasons and their
425   differences. DAOD is not only higher over the MDR in the high Caribbean DAOD seasons, but
426   dust aerosols are transported farther to the west. DAOD differences between the extreme high
427   and low DAOD seasons over the tropical North Atlantic and Caribbean are ~0.05-0.08. In fact,
428   the three high dust years have roughly 60% more DAOD in the Caribbean than the three low
429   dust years (regional average of 0.13 vs. 0.08), while these differences are not as large in the
430   tropical North Atlantic. The transport pathway of dust is also shifted slightly to the south in the
431   tropical North Atlantic in the three high DAOD seasons.

432   The right column of Figure 6 displays the JJA-averaged 850 hPa winds and 700 hPa RH for the
433   three high and three low JJA Caribbean DAOD seasons, and the difference between these high
434   and low seasons. Large-scale conditions over the Caribbean during JJA were much less
435   conducive for TCs in the high DAOD seasons, with drier middle levels (>10% relative humidity
436   difference) and stronger easterly trade winds (2-4 m s^{-1} stronger), implying an overall less
437   hurricane-favorable dynamic and thermodynamic environment. This is consistent with the
438   depiction of the thermodynamic structure of the SAL by Dunion and Velden (2004). The
439   stronger AEJ associated with higher DAOD is also consistent with modeling studies when
440   aerosol radiative effects are taken into account (Tompkins et al., 2005). Associated with high
441   Caribbean DAOD, the position of the center of the Azores High was slightly shifted to the
442   southwest, which facilitates stronger dust transport into the Caribbean. This is in agreement with
443   the findings of Riemer and Doherty (2006) who suggested the importance of the position of the
444   Azores High in African dust transport across the Atlantic, although their study was only during

445 the boreal winter. As would be expected from these large-scale conditions, Atlantic TC activity
446 was much higher in low JJA Caribbean DAOD seasons.

447 Table 2 displays observed Atlantic TC activity as well as the ratios of observed average seasonal
448 Atlantic TC activity in the three low JJA Caribbean DAOD seasons versus the three high
449 Caribbean DAOD seasons. Atlantic basin-wide numbers of tropical depressions, named storms,
450 hurricanes, major (Category 3+ on the Saffir-Simpson Hurricane Wind Scale) hurricanes and
451 ACE are higher by a factor of ~1.9 - ~2.8 in the three low relative to the three high Caribbean
452 DAOD seasons. The ratios are even higher (e.g., 12 times higher for ACE) for TC activity in the
453 Caribbean. The 2018 Atlantic hurricane season was an interesting case, as it was an above-
454 average overall hurricane season (as measured by ACE), but much of the ACE that was
455 generated that year occurred outside of the tropics (>23.5°N) (Saunders et al. 2020). Very little
456 activity occurred in the Caribbean in 2018.

457 In addition, the ratio for major hurricanes is higher than the ratios for tropical depressions,
458 named storms, and hurricanes, indicating a stronger relationship between dust aerosols and
459 intense storms than between dust aerosols and weak storms. A total of 17 major hurricanes were
460 observed in the Atlantic in the three low Caribbean DAOD seasons, compared with only 6 major
461 hurricanes in the three high Caribbean DAOD seasons. The three low Caribbean DAOD seasons
462 had six continental United States major hurricane landfalls (2005 Hurricanes Dennis, Katrina,
463 Rita, and Wilma and 2017 Hurricanes Harvey and Irma), while the three high Caribbean DAOD
464 seasons had one continental United States major hurricane landfall (2018 Hurricane Michael).

465 Figure 7 displays the named storm formation location of all Atlantic TCs in the three seasons
466 with the highest JJA Caribbean DAOD and the three seasons with the lowest Caribbean DAOD
467 along with the maximum intensity that these TCs reached. As would be expected from the
468 differences in large-scale conditions noted earlier, TCs that became major hurricanes formed
469 much more frequently south of 20°N in the three lowest Caribbean DAOD seasons than in the
470 three highest Caribbean DAOD seasons. These differences were most pronounced in the
471 Caribbean, with only one named storm (Hanna in 2014) forming in the Caribbean in the three
472 highest JJA Caribbean DAOD seasons. In the three lowest Caribbean JJA DAOD seasons, 11
473 named storms formed in the Caribbean.

474 **3.3 Relationship between JJA DAOD and large-scale atmosphere/ocean fields**

475 We next examine the relationship between JJA DAOD and large-scale atmosphere/ocean fields.
476 In this analysis, we begin by focusing on several fields that have been documented in prior
477 research to significantly impact Atlantic TC activity: 850 hPa zonal wind (850 hPa U), 200 hPa
478 zonal wind (200 hPa U), zonal wind shear between 200 hPa and 850 hPa, 700 hPa RH, 850 hPa
479 relative vorticity and SST (Gray, 1968; Saunders et al., 2017). More active Atlantic hurricane
480 seasons are typically associated with anomalous westerly 850 hPa U (e.g., weaker trade winds),
481 anomalous easterly 200 hPa U (counteracting prevailing upper-level westerlies) and thus weaker
482 wind shear, higher 850 hPa relative vorticity, higher mid-level relative humidity and
483 anomalously warm SSTs. We investigate the relationships with DAOD in the tropical North
484 Atlantic and the Caribbean as defined in Figure 2.

485 Figure 8 displays the correlation between regionally-averaged MRC JJA DAOD in the Caribbean
486 and the six large-scale fields just discussed. Higher JJA Caribbean DAOD is associated with

487 stronger 850 hPa easterly trades and increased 200 hPa upper-level westerlies (and hence
488 stronger vertical wind shear), drier air at 700 hPa and anomalously cool SST across the MDR.
489 Weaker 850 hPa relative vorticity also predominates over most of the Caribbean. However,
490 almost no correlation is found between Caribbean JJA DAOD and 850 hPa relative vorticity in
491 the tropical North Atlantic, possibly due to the counteracting role of covariability of African dust
492 emissions and AEWs - as was inferred from a positive correlation between the two by
493 Karyampudi and Carlson (1988). This result is also consistent with Figure 7 which shows more
494 named storms and therefore likely stronger AEW activity right off of the coast of west Africa
495 between 10-20°N in high dust DAOD years. This result reflects the complexity of the TC-dust
496 interaction relationship. In addition, the vorticity field is extremely noisy. Figure 8f is extended
497 to include the eastern and central tropical Pacific in order to investigate the potential relationship
498 between ENSO and DAOD, with Caribbean DAOD showing a significant positive relationship
499 with ENSO.

500 The relationship between the same six large-scale fields and JJA tropical North Atlantic DAOD
501 is considerably weaker, with lower correlations observed for all six fields (Figures S2). In
502 addition, the regions with significant correlations decrease in spatial extent relative to the
503 Caribbean DAOD correlations shown in Figure 8.

504 We next investigate Maximum Potential Intensity (MPI), an integrated TC index, which
505 combines a list of key factors (similar to those explored above). MPI assesses how conducive
506 atmospheric thermodynamic conditions are for TC intensification, providing a theoretical limit of
507 the strength of a TC (Holland, 1997; Bister and Emanuel, 1998). Figures 9a and c show the
508 correlations between the Caribbean region-averaged JJA DAOD and JJA/ASO MPI calculated
509 based on Bister and Emanuel (1998). Consistent with the results for the individual large-scale
510 fields, JJA MPI over the MDR exhibits strong negative correlations with JJA Caribbean DAOD
511 (~ -0.7, also Table 3). One of the primary inputs to the MPI calculation is SST, so the strong
512 inverse relationship between MPI and DAOD is expected given the strong inverse relationship
513 between SST and DAOD. The correlation is significant but weaker for ASO MPI for most of the
514 MDR, except for the eastern tropical North Atlantic, where the negative correlation drops below
515 statistical significance. The negative correlation of JJA/ASO MPI with JJA tropical North
516 Atlantic region-averaged DAOD is much weaker than that with JJA Caribbean DAOD in the
517 MDR (Figure 9b and d) and drops below statistical significance in the Caribbean.

518 The genesis potential index (GPI) is another integrated TC index that is often used to provide an
519 estimate of the potential for tropical cyclogenesis (e.g., Emanuel and Nolan, 2004; Camargo et
520 al., 2007). Monthly GPI is calculated following Emanuel and Nolan (2004). Figure 10 shows the
521 correlation between region-averaged JJA DAODs and JJA and ASO GPI. Consistent with the
522 results for the individual large-scale fields and MPI, JJA GPI over the MDR exhibits strong
523 negative correlations (~-0.7, also Table 3) with JJA Caribbean DAOD. Similar to MPI, GPI is
524 also directly related to SST via the potential intensity term, so given the negative correlation
525 between DAOD and SST, we would expect a negative correlation between GPI and DAOD.
526 Other terms also comprise the GPI, including vertical wind shear and mid-level moisture, which
527 also correlate negatively with DAOD. The correlation remains statistically significant but is
528 weaker for ASO GPI for most of the MDR. The exception is the eastern tropical North Atlantic,
529 where the negative correlation drops below 95% statistical significance. The negative correlation
530 of JJA/ASO GPI with JJA tropical North Atlantic region-averaged DAOD is much weaker than

531   that with JJA Caribbean DAOD in the MDR (Figure 10b and d), which is also consistent with the
532   result for the individual large-scale fields and MPI.

533   Table 3 summarizes the relationship between large-scale atmosphere/ocean fields, MPI, GPI, and
534   DAOD, with correlations displayed between JJA region-averaged DAOD and concurrent region-
535   averaged fields (i.e., JJA-averaged), as well as the large-scale region-averaged fields during the
536   peak of the Atlantic hurricane season from August-October. 850 hPa relative vorticity is
537   excluded as no statistically significant correlations are found. While the correlations between the
538   other five large-scale fields, MPI, GPI, and DAOD tend to weaken from JJA to ASO, the
539   correlations remain significant for all of these large-scale fields, and the integrated TC indices, in
540   the Caribbean during ASO. For the tropical North Atlantic, JJA DAOD has much weaker and
541   insignificant correlations with JJA 200 hPa zonal wind, wind shear and 700 hPa RH compared to
542   those for the Caribbean. However its negative correlation with SST is as strong as that for the
543   Caribbean in JJA and remains statistically significant from JJA to ASO, although the magnitude
544   of the correlation is weaker in ASO. These contribute to a negative correlation with MPI and GPI
545   and a stronger correlation during JJA than during ASO.

546   Part of the reason for the rapid decrease in the strength of the correlations in the tropical North
547   Atlantic is due to relatively low correlations between JJA and ASO values of large-scale
548   parameters in that portion of the basin, indicating a lack of persistence in atmosphere/ocean
549   conditions when compared with the Caribbean (Table 4). The persistence of the 700 hPa RH and
550   850 hPa U fields in the tropical North Atlantic is especially low compared to other fields.

551   **3.4 Relationship between JJA DAOD and large-scale climate modes**

552   We next explore the relationship between JJA-averaged DAOD and two large-scale climate
553   modes that have been documented in many studies to impact Atlantic TC activity: ENSO (e.g.,
554   Gray, 1984; Goldenberg & Shapiro, 1996; Klotzbach, 2011; Klotzbach et al., 2018) and the
555   AMM (e.g., Kossin & Vimont, 2007; Patricola et al., 2014). El Niño typically reduces Atlantic
556   TC activity through several mechanisms including increasing westerly wind shear especially
557   over the Caribbean (Gray, 1984) and through upper-level tropospheric warming, causing
558   increased static stability and inhibiting deep convection (Tang & Neelin, 2004). The AMM has
559   also been suggested in prior research to significantly impact Atlantic TC activity (Kossin &
560   Vimont, 2007), especially when combined with ENSO (Patricola et al., 2014). A positive phase
561   of the AMM is associated with a warmer than normal tropical Atlantic, anomalously low sea
562   level pressure and anomalously weak trade winds - all of which favor Atlantic TC formation
563   (Kossin & Vimont, 2007).

564   Table 5 displays the correlations between JJA regionally-averaged DAODs from the different
565   aerosol reanalysis products and the JJA and ASO ENSO (as represented by the ONI) and AMM
566   indices. There is a positive correlation between JJA Caribbean DAOD and the concurrent
567   (significant at the 90% level) and ASO ONI (significant at the 95% level) using MRC and
568   NAAPS-RA, and the correlations with the ONI increase from JJA to ASO. The correlation
569   between JJA tropical North Atlantic DAOD and JJA/ASO ENSO is not significant, however,
570   consistent with previous studies (Lau and Kim, 2007; Doherty et al., 2014). ENSO events
571   climatologically intensify from boreal summer to boreal autumn (Harrison & Larkin, 1998),
572   which may be part of the reason for the increase in significance of the correlations from JJA to
573   ASO. In addition, this likely also explains part of the reason why Atlantic TC activity correlates

574   more strongly with Caribbean DAOD than with tropical Atlantic DAOD, given the pronounced
575   impact that ENSO has on the Caribbean large-scale environment (Gray, 1984). Figure S3, in
576   which JJA composites of MRC DAOD, 850 hPa horizontal wind and 700 hPa RH for the three
577   top El Nino and La Nino ENSO years (based on JJA ONI) are shown, corroborates that stronger
578   dust transport into Caribbean occurs during El Nino years without necessarily strong emissions
579   over Africa and high DAOD over tropical North Atlantic. We also note that 2015 is both an El
580   Niño and a high DAOD year, while 2011 is both a La Niña and low DAOD year. Removing the
581   two overlapping years in the composites leads to similar results except that DAOD differences
582   between El Nino and La Nino years are more negative in the tropical North Atlantic, additionally
583   supporting the insignificant correlation between ENSO and tropical North Atlantic DAOD.

584   The correlations between JJA Caribbean DAOD and JJA AMM are consistently strong and
585   negative (~-0.7) with all of the aerosol reanalyses (Table 5). As might be expected given that the
586   signal of the AMM is climatologically strongest in the boreal spring and weakens in the boreal
587   summer and fall (Kossin & Vimont, 2007), correlations of JJA DAOD are weaker with the ASO
588   AMM than with the JJA AMM. Negative correlations are also obtained between the JJA tropical
589   North Atlantic DAOD and the JJA AMM, while the correlation with the ASO AMM is weak and
590   not statistically significant in general. The negative correlations between JJA DAODs and the
591   AMM are consistent with Evan et al. (2011)'s study on the radiative effect of dust aerosols on
592   the AMM. That study showed DAOD to be not only negatively correlated with the AMM but
593   that its variability was found to excite the AMM on interannual to decadal time scales.

594   So far we have shown that Caribbean DAOD is correlated with Atlantic basin-wide ACE as well
595   as two-large scale climate modes: ENSO and the AMM. Both of these modes have been shown
596   to also impact Atlantic TC activity. To remove the influence of these climate indices from the
597   relationship between DAOD and ACE, we use partial correlation analysis (Sharma et al., 1978).
598   Table 6 shows the partial correlation matrix between JJA Caribbean and tropical North Atlantic
599   DAOD and annual Atlantic basin-wide ACE while controlling for the ONI and AMM indices,
600   respectively. Removing the influence of ENSO causes little change in the negative correlation
601   between MRC Caribbean JJA DAOD and ACE. The correlation remains statistically significant,
602   suggesting that ENSO is not primarily responsible for the negative correlation between
603   Caribbean DAOD and Atlantic ACE, at least during the study period. The correlation between
604   tropical North Atlantic JJA DAOD and ACE also changes little, although the correlation is weak
605   and not statistically significant initially. We note that the correlation between ONI and ACE is
606   very weak and is not significant during the 2003-2018 study period, partially due to the
607   extremely active 2004 Atlantic hurricane season which occurred despite a weak El Niño event.

608   In contrast to the findings of removing ENSO from the DAOD-ACE relationship, after removing
609   the influence of the AMM, the correlation between Caribbean JJA DAOD and Atlantic ACE is
610   much weaker and drops to insignificant levels, suggesting that the AMM is an important factor in
611   the dust-TC relationship. However, it is hard to argue that the AMM is the determining factor in
612   the dust-TC relationship, as the correlation of ACE with JJA Caribbean DAOD is slightly higher
613   than with the JJA AMM (-0.61 vs. 0.59). When the partial correlation is calculated between the
614   AMM and ACE while removing the Caribbean dust (DAOD) influence, the correlation drops
615   from 0.59 to an insignificant level (r = ~0.26), independent of season examined. This indicates
616   that Caribbean DAOD is, in turn, an important factor in the AMM-TC relationship. When the
617   TATL JJA DAOD is removed, the correlation between AMM and ACE is also reduced, implying

618 that the AMM/DAOD/TC relationship is strongly intertwined. This is physically feasible, as the
619 dust radiative forcing can result in cooler SST, which can introduce anomalously high sea level
620 pressure and stronger trade winds (and therefore stronger vertical wind shear), which is
621 characteristic of a negative AMM. This air-sea coupled response to dust radiative forcing can act
622 over relatively short timescales (e.g., one to two months) (Evan et al. 2011). Additionally, the
623 dryness of the dusty air and the radiative heating of the dust layer, can lead to stronger vertical
624 wind shear and a more stable lower atmosphere, all in line with a negative AMM that creates an
625 environment that is detrimental for TC formation and development. It could be argued that the
626 negative correlation between DAOD and Atlantic TC activity may be a result of forcing of the
627 AMM by African dust.

628 **4. Sensitivity tests**

629 The sensitivity of our results to the domain definitions of the tropical North Atlantic and the
630 Caribbean regions is explored by defining equal areas (shifting the separation longitude to
631 52.5°W) for the two regions within the MDR, as well as by expanding the two regions by 5°
632 latitude to the north (e.g., to 25°N). Neither of the two new definitions for regions significantly
633 change the correlations between JJA regionally averaged DAOD and large-scale fields (Table
634 S1, S2). The correlations between the JJA Caribbean DAOD and ACE are -0.59/-0.58 for the
635 longitudinal and latitudinal shift respectively, only slightly lower than -0.61 using the default
636 regional definitions. The correlations between the JJA TATL DAOD and ACE remain
637 insignificant (Table S3).

638 While airborne dust can impact TC activity, once TCs form and develop, both precipitation and
639 strong winds can significantly remove these dust particles. However, the removal effect by TCs
640 cannot primarily explain the negative DAOD-TC relationship. This is because peak dust activity
641 occurs from June to August with larger DAOD in June and July than in August over the Atlantic,
642 suggesting that peak DAOD in general leads the peak TC season by ~1-2 months (Figure S1).
643 Using June-July average DAOD instead of June-August average DAOD changes our results only
644 slightly. For example, the correlation between June-July Caribbean DAOD and Atlantic ACE is -
645 0.58, only slightly lower than that using JJA DAOD ($r = -0.61$) (Table S3). This has implications
646 for using DAOD as an indicator for seasonal TC forecasts which are often updated in early
647 August.

648 The sensitivity of the composite analysis of high versus low JJA Caribbean DAOD years to the
649 number of years is also explored by using two and four years for composites in addition to three
650 years (Table S4). Consistent results are found across all sensitivity tests. Atlantic basin-wide
651 numbers of tropical depressions, named storms, hurricanes and major hurricanes, and ACE are
652 higher (by a factor of 1.6-5) in the low than in the high JJA Caribbean DAOD seasons. The ratios
653 of observed average seasonal Atlantic hurricanes and major hurricanes in the low versus the high
654 JJA Caribbean DAOD seasons are generally higher than those of tropical depressions and named
655 storms, suggesting a stronger correlation relationship between dust aerosols and intense storms
656 than weak storms.

657 **5. Conclusions and Discussions**

658 The relationship between African dust and Atlantic tropical cyclone (TC) activity has been
659 analyzed in many prior studies (e.g., Dunion & Velden 2004; Evan et al. 2006a; Braun et al.

16

660 2013; Pan et al. 2018). This study has revisited this relationship with a statistical analysis using
661 three newly available aerosol reanalyses: the Naval Aerosol Analysis and Prediction System
662 reanalysis (NAAPS-RA), the Modern-Era Retrospective analysis for Research and Applications,
663 Version 2 (MERRA-2) aerosol reanalysis, the Copernicus Atmosphere Monitoring Service
664 ReAnalysis (CAMSRA), and a multi-reanalysis-consensus (MRC) based on the three reanalyses
665 for the period 2003-2018. The datasets are validated with ground-based observations for modal
666 (fine, coarse and total) aerosol optical depth (AOD). The MRC data is primarily used in this
667 study as it generally has better verification results than any of the individual reanalysis products.
668 To our knowledge, this is the first climate study using a multi-reanalysis consensus to represent
669 aerosol conditions. Our findings are summarized below:

670 1. Total AOD of the three aerosol reanalysis products are similar for the Atlantic Main
671   Development Region, however, AOD attributed to individual aerosol species (such as
672   dust aerosols) can be quite different among the three reanalysis products (Figure 4). June-
673   July-August (JJA) dust AOD (DAOD) magnitude can differ by as much as 0.06,
674   corresponding to approximately 60% of the climatological JJA DAOD based on MRC for
675   the Caribbean, and can differ by as much as 0.05, approximately 20% of the
676   climatological JJA DAOD based on MRC for the tropical North Atlantic. This is because
677   total AOD is the only aerosol property constrained by satellite observations through AOD
678   data assimilation in all three aerosol reanalysis products, while speciated AOD is not
679   constrained. This also supports the potential usefulness of MRC, as multi-model-
680   consensus are found to generally be better performers than individual models in aerosol
681   simulations (Sessions et al., 2015; Xian et al., 2019). Despite differences in DAOD
682   magnitude, DAODs of the three reanalysis products correlate significantly over the
683   tropical Atlantic and Caribbean.

684 2. Each of the three individual reanalyses and the MRC have significant and negative
685   correlations between JJA Caribbean DAOD and seasonal Atlantic Accumulated Cyclone
686   Energy (ACE) (Table 2). High JJA DAOD in the Caribbean is associated with a less
687   conducive environment for hurricane activity as represented by cooler SST, enhanced
688   vertical wind shear, lower mid-level moisture, and by lower Maximum Potential Intensity
689   (MPI) and Genesis Potential Index (GPI) values (Table 3). Pronounced differences in
690   Atlantic TC activity are seen when examining the three seasons with the highest levels of
691   JJA Caribbean DAOD compared with the three seasons with the lowest JJA Caribbean
692   DAOD (Table 4 and Figure 7). About three times as many major hurricanes occurred
693   during the three lowest DAOD seasons (2005, 2011, 2017) compared with the three
694   highest DAOD seasons (2018, 2015, 2014). Atlantic TC activity is also negatively
695   correlated with tropical North Atlantic DAOD but not as significantly as with Caribbean
696   DAOD for possible reasons discussed in the conclusion that follows.

697 3. High Caribbean DAOD is typically associated with El Niño conditions, however ENSO
698   does not appear to significantly impact the Caribbean DAOD-ACE relationship. The
699   robust DAOD-ACE correlation still holds after removing ENSO's influence via partial
700   correlation analysis.

701 4. JJA north Atlantic DAOD and the Atlantic Meridional Mode (AMM) are intertwined in
702   the dust-TC relationship. Both the Caribbean and tropical North Atlantic DAODs have
703   strong negative correlations with JJA values of the AMM index (with a stronger

17

704   correlation for the Caribbean DAOD). Meanwhile, the JJA AMM index correlates
705   significantly with Atlantic ACE. For AMM and DAOD, removing the other in their
706   relationships with ACE dramatically reduces the significance of the correlations based on
707   partial correlation analysis. This result supports Evan et al.(2011)'s work, which showed
708   that African dust excited AMM variability on interannual to decadal time scales through
709   radiative forcing of the underlying SST. Consequently, it can be argued that the negative
710   correlation between Caribbean and tropical North Atlantic DAOD and Atlantic TC
711   activity may be a result of forcing of the AMM by African dust.

712 These results agree with previous studies that showed negative correlations between boreal
713 summer Atlantic dustiness and TC activity (e.g., Dunion and Velden, 2004; Evan et al., 2006a;
714 Lau and Kim 2007). The correlations obtained in this study, especially those with Caribbean
715 DAOD, are slightly higher than previous studies, including correlations between boreal summer
716 dustiness and ACE (Evan et al., 2006a; Lau and Kim 2007) and between JJA dustiness and
717 ENSO (DeFlorio et al., 2016). We note that the study areas, time periods and study methods are
718 not identical between our study and these previous studies, implying the usefulness of aerosol
719 reanalyses in climate studies. Various sensitivity tests show that our results are not sensitive to
720 the definitions of areas for the Caribbean and tropical North Atlantic, the number of composite
721 years used, or the definition of the dust season (June-July vs. June-August).

722 Our results also document statistically significant relationships between Atlantic dustiness and
723 large-scale fields (e.g., SST, vertical wind shear, mid-level moisture and relatively vorticity) and
724 integrated TC diagnostic indices (e.g., MPI and GPI), which can be seen as confounding factors
725 in the dust-TC relationship. Exploring the causality of the documented negative correlation
726 between DAOD and Atlantic TC activity through modeling experiments is beyond the scope of
727 this paper. However in some modeling studies, radiative forcing of the scattering dust alone
728 could result in an inverse relationship between African dust and Atlantic TC activity (Dunstone
729 et. al, 2013; Strong et al., 2018; Sobel et al., 2019), along with consistent large-scale fields
730 associated with TC activity. So it is possible that radiative forcing of the scattering dust is a
731 dominant factor in the inverse dust-TC relationship on seasonal-interannual and basin-wide
732 scales. After all, aerosols are coupled radiatively with meteorology in the ERA-Interim dataset,
733 which provides the large-scale atmospheric data used in this study.

734 The correlations with Atlantic ACE are higher for Caribbean DAOD than for tropical North
735 Atlantic DAOD - a result that was not documented previously. The differences in the
736 relationships of Atlantic ACE with regional DAOD are potentially due to several factors:

737 a)   The large-scale environmental fields investigated herein are better self-correlated
738 between the JJA and ASO seasons over the Caribbean than over the tropical North Atlantic
739 (Table 4). Therefore, the higher correlation with JJA Caribbean DAOD, which reflects the large-
740 scale circulation, especially for the low- and mid-level wind flow that modulates how far African
741 dust can be transported, tends to extend into the ASO peak TC season. As was shown in
742 Saunders et al. (2017), the strength of the low-level winds in the Caribbean tends to be the most
743 robust diagnostic for seasonal ACE during the peak months of the Atlantic hurricane season.

744 b)   ENSO has a large impact on the Caribbean large-scale environment (Gray, 1984). ENSO-
745 forced SST anomalies typically exhibit very strong persistence from JJA to ASO (Harrison &

746 Larkin, 1998). As Caribbean JJA DAOD is correlated with ENSO to some extent, it is also
747 correlated with Atlantic ACE.

748 c)   There might be a regime shift in the integrated outcome of dust-TC interactions from east
749 to west across the tropical North Atlantic at climate time scales, with the eastern tropical North
750 Atlantic (e.g., close to the African continent) having a positive correlation (e.g., since dust
751 emission is often associated with AEWs emerging from Africa; Jones et al., 2003; Karyampudi
752 and Carlson, 1988) while the correlation becomes more negative heading west across the basin.

753 d)   The relatively larger JJA DAOD variability in the Caribbean (larger relative dynamical
754 range of Caribbean JJA DAOD compared to the tropical north Atlantic JJA DAOD over 2003-
755 2018) could contribute to a higher correlation (Figures 3 and 4).

756 e)   AOD data quality is comparatively better over the Caribbean than over the tropical north
757 Atlantic (Table 1; Figure 3), given that AOD reanalyses generally perform better over long-range
758 transport regions than they do closer to the aerosol source regions (Xian et al., 2016).

759 The conclusions drawn from this study are based on 16-year records (2003-2018) of DAOD data
760 from the MRC. We acknowledge that this analysis represents a relatively short timespan for a
761 climate correlation study. Longer-period aerosol reanalyses with good fidelity are needed for
762 further climate studies. These reanalyses face several challenges including dealing with changes
763 to the network of AOD-observing satellites over time, as well as reasonable simulations and
764 partitioning of aerosol-speciated AODs associated with rare severe aerosol events (e.g., volcanic
765 eruptions) within AOD data assimilation systems.

766 It is also worth noting that the 2003-2018 DAOD climatology for the Atlantic MDR could be
767 low relative to the extremely dusty period of the 1980s that has been documented by long-term
768 in-situ dust concentration measurements made in Barbados (Prospero, 2014) and a 24-year
769 eastern North Atlantic dust cover record derived from the Advanced Very High Resolution
770 Radiometer (AVHRR, Evan et al., 2006). Dust concentration records at Barbados (1965-2011)
771 and dust cover determined from AVHRR (1982-2005) both indicate that dust levels over the
772 North Atlantic peaked during the mid-1980s, when tropical Atlantic TC activity was relatively
773 low (e.g., Wang et al., 2012). Our findings are consistent with the negative correlations reflected
774 in both the earlier dust and the earlier tropical Atlantic TC activity records.

775 Since we note that JJA/JJ Caribbean DAOD are strongly correlated with large-scale atmospheric
776 fields which are frequently used in seasonal hurricane forecasts, DAOD may be a useful
777 confirmation tool for observed thermodynamic conditions. Most groups issuing seasonal
778 hurricane forecasts provide an update in early August (immediately prior to the peak of the
779 Atlantic hurricane season). So early season (June-July) DAOD, especially over the Caribbean,
780 could be a potential indicator for the strength of seasonal Atlantic TC activity. While there is
781 very strong agreement between large-scale zonal wind fields (e.g., the June-July-averaged 850
782 hPa zonal wind over the tropical Atlantic correlates at 0.92 between ERA-Interim and MERRA-
783 2, in which impact of aerosols on radiation and thereby on meteorology is included), there is less
784 agreement with the mid-level moisture field. The correlation between ERA-Interim and
785 MERRA-2 700 hPa RH over the tropical Atlantic averaged over June-July is only 0.72. The
786 DAOD could potentially be used to help clarify the favorability/unfavorability of the

787 thermodynamic environment, as indicated also by the strong correlation between JJA Caribbean
788 DAOD and JJA and ASO MPI.

789 We believe this study, which shows a robust correlation relationship for the integrated dust-
790 atmosphere-ocean system, could provide a framework to better understand the linkages between
791 DAOD and Atlantic TC activity and how DAOD affects the large-scale environment of the
792 MDR. This study focuses on seasonal to interannual time scales and provides aspects from a
793 large-scale point of view. Finer temporal scales (from hours to days) are needed in future studies
794 for cases where African dust is entrained into TC vortices.

801 **Data Availability:** All data supporting the conclusions of this manuscript are available through
802 the links provided below:
803 AERONET Version 3 Level 2 data: http://aeronet.gsfc.nasa.gov
804 AMM index:
805 https://www.esrl.noaa.gov/psd/data/timeseries/monthly/AMM/ammsst.data
806 CAMSRA AOD: https://www.ecmwf.int/en/research/climate-reanalysis/cams-reanalysis
807 ENSO index:
808 http://origin.cpc.ncep.noaa.gov/products/analysis_monitoring/ensostuff/ONI_v5.php
809 ERA-interim monthly means: https://rda.ucar.edu/datasets/ds627.1/
810 HURDAT2:
811 https://www.aoml.noaa.gov/hrd/hurdat/hurdat2.html
812 MERRA-2 AOD:
813 https://disc.gsfc.nasa.gov/datasets/M2TMNXAER_V5.12.4/summary?keywords=%22MERRA-
814 2%22
815 NAAPS RA AOD: https://usgodae.org//cgi-
816 bin/datalist.pl?dset=nrl_naaps_reanalysis&summary=Go
817 NOAA OI SST V2 data: https://www.esrl.noaa.gov/psd/
818

819 **Author contribution:** P. J. K, J. P. D. and P.X. conceived the idea. P.X. and P.J.K performed
820 most of the analysis. M.A.J. calculated and performed the analyses on MPI and GPI. All authors
821 contributed to the writing and revision of the manuscript.
822

823 **Competing interests:** The authors declare that they have no conflict of interest.
824

825 **References**
826 Barnston, A. G., Chelliah, M., & Goldenberg, S. B. (1997). Documentation of a highly ENSO-
827 related SST region in the equatorial Pacific. *Atmosphere-Ocean,* 35(3), 367-383.
828 https://doi.org/10.1080/07055900.1997.9649597
829 Bell, G. D., Halpert, M. S., Schnell, R. C., Higgins, R. W., Lawrimore, J., Kousky, V. E., et al.
830 (2000). Climate assessment for 1999. *Bulletin of the American Meteorological Society,* 81(6),
831 S1-S50. https://doi.org/10.1175/1520-0477(2000)81[s1:CAF]2.0.CO;2

832 Bercos-Hickey, E., Nathan, T. R., and Chen, S. H. (2017). Saharan dust and the African easterly
833 jet-African easterly wave system: Structure, location and energetics. *Quarterly Journal of the*
834 *Royal Meteorological Society*, 143(708), 2797-2808. https://doi.org/10.1002/qj.3128
835 Bister, M., and Emanuel, K. A. (2002). Low frequency variability of tropical cyclone potential
836 intensity. 1. Interannual to interdecadal variability. *J. Geophys. Res*., 107, 4801,
837 doi:10.1029/2001JD000776.
838 Braun, S. A., Sippel, J. A., Shie, C.-L., & Boller, R. A. (2013). The evolution and role of the
839 Saharan air layer during Hurricane Helene (2006). *Monthly Weather Review,* 141(12), 4269–
840 4295. https://doi.org/10.1175/MWR-D-13-00045.1
841 Braun, S. A. (2010). Re-evaluating the role of the Saharan Air Layer in Atlantic tropical
842 cyclogenesis and evolution. *Monthly Weather Review,* 138(6), 2007–2037.
843 https://doi.org/10.1175/2009MWR3135.1
844 Bretl, S., Reutter, P, Raible, C. C., Ferrachat, S., Poberaj, C. S., Revell, L. E., & Lohmann, U.
845 (2015). The influence of absorbed solar radiation by Saharan dust on hurricane genesis. *Journal*
846 *of Geophysical Research: Atmospheres*, 120(5), 1902–1917.
847 https://doi.org/10.1002/2014JD022441.
848 Buchard, V., Randles. C. A., da Silva, A., Darmenov, A. S., Colarco, P. R., Govindaraju, R.C., et
849 al., (2017). The MERRA-2 Aerosol Reanalysis, 1980-onward, Part II: Evaluation and case
850 studies. *Journal of Climate*, 30(17), 6851-6872. https://doi.org/10.1175/JCLI-D-16-0613.1
851 Carlson, T. N., & Prospero, J. M. (1972). The large-scale movement of Saharan air outbreaks
852 over the northern equatorial Atlantic. *Journal of Applied Meteorology,* 11(2), 283–297.
853 https://doi.org/10.1175/1520-0450(1972)011<0283:TLSMOS>2.0.CO;2
854 Camargo, S. J., Emanuel, K. A. & Sobel, A. H. (2007). Use of a genesis potential index to
855 diagnose ENSO effects on tropical cyclone genesis. *J. Clim.* **20**, 4819–4834.
856 Chin, M., Rood, R., Lin, S., Muller J., & Thompson, A. (2000). Atmospheric sulfur cycle
857 simulated in the global model GOCART: Model description and global properties. *Journal of*
858 *Geophysical Research: Atmospheres,* 105(D20), 24,671–24,687.
859 https://doi.org/10.1029/2000JD900384
860 Colarco, P. R., Toon, O. B., Reid, J. S., Livingston, J. M., Russell, P. B., Redemann, J., et al.,
861 (2003). Saharan dust transport to the Caribbean during PRIDE: 2. Transport, vertical profiles,
862 and deposition in simulations of in situ and remote sensing observations. *Journal of Geophysical*
863 *Research: Atmospheres*, 108(D19), 8590, https://doi.org/10.1029/2002JD002659
864 Colarco, P., da Silva, A., Chin, M., & Diehl, T. (2010). Online simulations of global aerosol
865 distributions in the NASA GEOS-4 model and comparisons to satellite and ground-based aerosol
866 optical depth, *Journal of Geophysical Research: Atmospheres*, 115(D14207),
867 https://doi.org/10.1029/2009JD012820
868 Dee, D. P., Uppala, S. M., Simmons, A. J., Berrisford, P., Poli, P., Kobayashi, S., Andrae, U., et
869 al. (2011). The ERA-Interim reanalysis: configuration and performance of the data assimilation
870 system. *Quarterly Journal of the Royal Meteorological Society*, 137(656), 553-597.
871 https://doi.org/10.1002/qj.828
872 DeFlorio, M. J., Goodwin, I. D., Cayan, D. R., Miller, A. J., Ghan, S. J., Pierce, D. W., Russell,
873 L. M., et al. (2016). Interannual modulation of subtropical Atlantic boreal summer dust
874 variability by ENSO. *Climate Dynamics,* 46(1), 585-599. https://doi.org/10.1007/s00382-015-
875 2600-7

DeMott, P., Sassen, K., Poellot, M., Baumgardner, D., Rogers, D., Brooks, S. D., Prenni, A. J., & Kreidenweis, S. M. (2003). African dust aerosols as atmospheric ice nuclei. *Geophysical Research Letters*, 30, 1732. https://doi.org/10.1029/2003GL017410

Doherty, O. M., Riemer, N., & Hameed, S. (2008). Saharan mineral dust transport into the Caribbean: Observed atmospheric controls and trends, *Journal of Geophysical Research: Atmospheres*, 113(D07211). https://doi.org/10.1029/2007JD009171

Dunion, J. P., (2011). Re-writing the climatology of the tropical North Atlantic and Caribbean Sea atmosphere. *Journal of Climate*, 24(3), 893–908. https://doi.org/10.1175/2010JCLI3496.1

Dunion, J. P., & Marron, C. S. (2008). A reexamination of the Jordan mean tropical sounding based on awareness of the Saharan air layer: Results from 2002. *Journal of Climate,* 21(20), 5242–5253. https://doi.org/10.1175/2008JCLI1868.1

Dunion, J. P., & Velden, C. S. (2004). The impact of the Saharan Air Layer on Atlantic tropical cyclone activity. *Bulletin of the American Meteorological Society,* 85(3), 353-365. https://doi.org/10.1175/BAMS-85-3-353

Emanuel, K. A., & Nolan, D. S. (2004). Tropical cyclone activity and global climate. In: *Proc. of 26th Conference on Hurricanes and Tropical Meteorology*, pp. 240–241, American Meteorological Society , Miami, FL.

Engelstaedter, S., & Washington, R. (2007). Atmospheric controls on the annual cycle of North African dust, *Journal of Geophysical Research: Atmospheres*, 112(D3), D03103. https://doi.org/10.1029/2006JD007195

Evan, A.T., Dunion, J. P., Foley, J. A., Heidinger, A. K., & Velden, C. S. (2006a). New evidence for a relationship between Atlantic tropical cyclone activity and African dust outbreaks. *Geophysical Research Letters,* 33, L19813. https://doi.org/10.1029/2006GL026408

Evan, A. T., Heidinger, A. K., & Knippertz P. (2006b). Analysis of winter dust activity off the coast of West Africa using a new 24-year over-water advanced very high resolution radiometer satellite dust climatology. *Journal of Geophysical Research: Atmospheres*, 111(D12), D12210. https://doi.org/10.1029/2005JD006336

Evan, A. T., Foltz, G. R., Zhang, D., & Vimont D. J. (2011). Influence of African dust on ocean–atmosphere variability in the tropical Atlantic. *Nature Geoscience*.4, 762–765. https://doi.org/10.1038/ngeo1276

Evan, A. T., Vimont, D. J., Heidinger, A. K., Kossin, J. P., & Bennartz, R. (2009). The role of aerosols in the evolution of tropical North Atlantic Ocean temperature anomalies. *Science,* 324(5928), 778-781. https://doi.org/10.1126/science.1167404

Flemming, J., Benedetti, A., Inness, A., Engelen, R. J., Jones, L., Huijnen, V., Remy, S., Parrington, M., Suttie, M., Bozzo, A., Peuch, V.-H., Akritidis, D., and Katragkou, E.: The CAMS interim Reanalysis of Carbon Monoxide, Ozone and Aerosol for 2003–2015, Atmos. Chem. Phys., 17, 1945–1983, https://doi.org/10.5194/acp-17-1945-2017, 2017.

Giles, D. M., Sinyuk, A., Sorokin, M. G., Schafer, J. S., Smirnov, A., Slutsker, I., Eck, T. F., et al. (2019). Advancements in the Aerosol Robotic Network (AERONET) Version 3 database – automated near-real-time quality control algorithm with improved cloud screening for Sun photometer aerosol optical depth (AOD) measurements. *Atmospheric Measurement Techniques*, 12(1), 169-209, https://doi.org/10.5194/amt-12-169-2019.

Goldenberg, S. B., Landsea, C. W., Mestas-Nuñez, A. M., & Gray, W. M. (2001). The recent increase in Atlantic hurricane activity: Causes and implications. *Science,* 293(5529), 474-479. https://doi.org/10.1126/science.1060040

Goldenberg, S. B., & Shapiro, L. J. (1996). Physical mechanisms for the association of El Niño and West African rainfall with Atlantic major hurricane activity. *Journal of Climate,* 9(6), 1169-1187. https://doi.org/10.1175/1520-0442(1996)009%3C1169:PMFTAO%3E2.0.CO;2

Gray, W. M. (1968). Global view of the origin of tropical disturbances and storms. *Monthly Weather Review,* 96(10), 669-700. https://doi.org/10.1175/1520-0493(1968)096%3C0669:GVOTOO%3E2.0.CO;2

Gray, W. M. (1984). Atlantic seasonal hurricane frequency. Part I: El Niño and 30 mb quasi-biennial oscillation influences. *Monthly Weather Review,* 112(9), 1649-1668. https://doi.org/10.1175/1520-0493(1984)112%3C1649:ASHFPI%3E2.0.CO;2

Grogan, D. F. P., Nathan, T. R., Chen, S. H. (2016). Effects of Saharan dust on the linear dynamics of African easterly waves. *Journal of Atmospheric Science,* 73(2), 891–911. https://doi.org/10.1175/JAS-D-15-0143.1

Grogan, D. F. P., Nathan, T. R., Chen, S. H. (2017). Saharan dust and the nonlinear evolution of the African easterly jet–African easterly wave system. *Journal of Atmospheric Science*, 74(1), 27–47. https://doi.org/10.1175/JAS-D-16-0118.1

Harrison, D. E., Larkin, N. K. (1998). El Niño-Southern Oscillation sea surface temperature and wind anomalies, 1946-1993. *Reviews of Geophysics,* 36(3), 353-400. https://doi.org/10.1029/98RG00715

Herbener, S. R., van den Heever, S. C., Carrio, G. G., Saleeby, S. M., Cotton W. R. (2014), Aerosol indirect effect on idealized tropical cyclone dynamics. *Journal of Atmospheric Science*, 71, 2040-2055. https://doi.org/10.1175/JAS-D-13-0202.1

Herbener, S. R., S. M. Saleeby, S. C. van den Heever, and C. H. Twohy (2016), Tropical storm redistribution of Saharan dust to the upper troposphere and ocean surface, *Geophys. Res. Lett*., 43, doi:10.1002/2016GL070262.

Holben, B. N., Eck, T. F., Slutsker, I., Tanre, D., Buis, J. P., Setzer, A., et al. (1998). AERONET - A federated instrument network and data archive for aerosol characterization, *Remote Sensing of the Environment*, 66(1), 1-16. https://doi.org/10.1016/S0034-4257(98)00031-5

Holben, B. N., Tanré, D., Smirnov, A., Eck, T. F., Slutsker, I., Abuhassan, N., et al. (2001). An emerging ground-based aerosol climatology: Aerosol optical depth from AERONET, *Journal of Geophysical Research: Atmospheres,* 106(D11), 12067-12097. https://doi.org/10.1029/2001JD900014

Holland, G. J., 1997: The maximum potential intensity of tropical cyclones. *J. Atmos. Sci.*, **54**, 2519–2541, https://doi.org/10.1175/1520-0469(1997)054<2519:TMPIOT>2.0.CO;2

Hsu, N. C., Gautam, R., Sayer, A. M., Bettenhausen, C., Li, C., Jeong, M. J., et al. (2012). Global and regional trends of aerosol optical depth over land and ocean using SeaWiFS measurements from 1997 to 2010. *Atmospheric Chemistry and Physics,* 12, 8037-8053. https://doi.org/10.5194/acp-12-8037-2012

Hyer, E. J., Reid, J. S., & Zhang, J. (2011). An over-land aerosol optical depth data set for data assimilation by filtering, correction, and aggregation of MODIS Collection 5 optical depth retrievals. *Atmospheric Measurement Techniques*, 4(3), 379-408. https://doi.org/10.5194/amt-4-379-2011

Inness, A., Baier, F., Benedetti, A., Bouarar, I., Chabrillat, S., Clark, H., Clerbaux, C., Coheur, P., Engelen, R. J., Errera, Q., Flemming, J., George, M., Granier, C., Hadji-Lazaro, J., Huijnen, V., Hurtmans, D., Jones, L., Kaiser, J. W., Kapsomenakis, J., Lefever, K., Leitão, J., Razinger, M., Richter, A., Schultz, M. G., Simmons, A. J., Suttie, M., Stein, O., Thépaut, J.-N., Thouret, V., Vrekoussis, M., Zerefos, C., and the MACC team: The MACC reanalysis: an 8 yr data set of

23

atmospheric composition, Atmos. Chem. Phys., 13, 4073–4109, https://doi.org/10.5194/acp-13-4073-2013, 2013.

Inness, A., Ades, M., Agustí-Panareda, A., Barré, J., Benedictow, A., Blechschmidt, A.-M., Dominguez, J. J., Engelen, R., Eskes, H., Flemming, J., Huijnen, V., Jones, L., Kipling, Z., Massart, S., Parrington, M., Peuch, V.-H., Razinger, M., Remy, S., Schulz, M., and Suttie, M.: The CAMS reanalysis of atmospheric composition, Atmos. Chem. Phys., 19, 3515–3556, https://doi.org/10.5194/acp-19-3515-2019, 2019.

Jenkins, G. S., Pratt, A. S. & Heymsfield, A. (2008). Possible linkages between Saharan dust and tropical cyclone rain band invigoration in the eastern Atlantic during NAMMA-06. *Geophysical Research Letters*, 35, L08815. https://doi.org/10.1029/2008GL034072

Jones, T. A., Cecil, D. J. & Dunion, J. (2007). The environmental and inner-core conditions governing the intensity of Hurricane Erin (2001). *Weather and Forecasting*, 22(4), 708–725. https://doi.org/10.1175/WAF1017.1

Jones, C., Mahowald, N. M., & Luo, C. (2003). The role of easterly waves on African desert dust transport. *Journal of Climate*, 16, 3617-3628.

Jones, C., Mahowald, N. M., & Luo, C. (2004). Observational evidence of African desert dust intensification of easterly waves. *Geophysical Research Letters*, 31(17), L17208. https://doi.org/10.1029/2004GL020107.

Joyce, R. J., Janowiak, J. E., Arkin, P. A., Xie, P. (2004). CMORPH: A method that produces global precipitation estimates from passive microwave and infrared data at high spatial and temporal resolution. *Journal of Hydrometeorology,* 5(3), 487-503, https://doi.org/10.1175/1525-7541(2004)005%3C0487:CAMTPG%3E2.0.CO;2

Kahn, R. A., & Gaitley, B. J. (2015). An analysis of global aerosol type as retrieved by MISR. *Journal of Geophysical Research: Atmospheres*, 120(9), 4248–4281. https://doi.org/10.1002/2015JD023322

Kaku, K. C., Reid, J. S., O'Neill, N. T., Quinn, P. K., Coffman, D. J., & Eck, T. F. (2014). Verification and application of the extended spectral deconvolution algorithm (SDA+) methodology to estimate aerosol fine and coarse mode extinction coefficients in the marine boundary layer. *Atmospheric Measurement Techniques*, 7(10), 3399-3412. https://doi.org/10.5194/amt-7-3399-2014

Karyampudi, V. M., & Carlson, T. N. (1988). Analysis and numerical simulations of the Saharan air layer and its effect on easterly wave disturbances. *Journal of the Atmospheric Sciences,* 45(21), 3102–3136. https://doi.org/10.1175/1520-0469(1988)045<3102:AANSOT>2.0.CO;2

Karyampudi, V. M., & Pierce, H. F. (2002). Synoptic-scale influence of the Saharan Air Layer on tropical cyclogenesis over the eastern Atlantic. *Monthly Weather Review*, 130, 3100-3128.

Karydis, V. A., Kumar, P., Barahona, D., Sokolik, I. N. & Nenes, A. (2011). On the effect of dust particles on global cloud condensation nuclei and cloud droplet number. *Journal of Geophysical Research: Atmospheres*, 116(D23204). https://doi.org/10.1029/2011JD016283

Khain, A. P., Leung, L. R., Lynn, B., & Ghan, S. (2009). Effects of aerosols on the dynamics and microphysics of squall lines simulated by spectral bin and bulk parameterization schemes. *Journal of Geophysical Research: Atmospheres*, 114(D22203). https://doi.org/10.1029/2009JD011902

Klotzbach, P. J. (2011). El Niño – Southern Oscillation's impact on Atlantic basin hurricanes and U.S. landfalls. *Journal of Climate,* 24(4), 1252-1263. https://doi.org/10.1175/2010JCLI3799.1

Klotzbach, P. J., Bowen, S. G., Pielke Jr., R., Bell, M. M. (2018). Continental United States landfall frequency and associated damage. Observations and future risks. *Bulletin of the*

American Meteorological Society, 99(7), 1359-1376. https://doi.org/10.1175/BAMS-D-17-0184.1

Knippertz, P., Todd, M. C. (2010). The central west Saharan dust hot spot and its relation to African easterly waves and extratropical disturbances. *Journal of Geophysical Research: Atmospheres*, 115(D12117). https://doi.org/10.1029/2009JD012819.

Kossin, J. P., & Vimont, D. J. (2007). A more general framework for understanding Atlantic hurricane variability and trends. *Bulletin of the American Meteorological Society,* 88(11), 1767–1782. https://doi.org/10.1175/BAMS-88-11-1767

Kuciauskas, A. P., Xian, P., Hyer, E. J., Oyola, M. I. & Campbell, J. R. (2018). Supporting weather forecasters in predicting and monitoring Saharan Air Layer dust events as they impact the Greater Caribbean. *Bulletin of the American Meteorological Society,* 99(2), 259-268. https://doi.org/10.1175/BAMS-D-16-0212.1

Landsea, C. W. (1993). A climatology of intense (or major) Atlantic hurricanes. *Monthly Weather Review,* 121(6), 1703-1713. https://doi.org/10.1175/1520-0493(1993)121%3C1703:ACOIMA%3E2.0.CO;2

Landsea, C. W., & Franklin, J. L. (2013). Atlantic hurricane database uncertainty and presentation of a new database format. *Monthly Weather Review,* 141(10), 3576-3592. https://doi.org/10.1175/MWR-D-12-00254.1

Lau, W. K. M., & Kim, K. (2007). How nature foiled the 2006 hurricane forecasts. *Eos Transactions American Geophysical Union,* 88(9), 105-107. https://doi.org/10.1029/2007EO090002

Levy, R. C., et al. (2005) Evaluation of the MODIS aerosol retrievals over ocean and land during CLAMS, *J. Atmos. Sci.*, 62(4), 974–992.

Levy, R. C., Remer, L. A., Kleidman, R. G., Mattoo, S., Ichoku, C., Kahn, R., & Eck, T. F. (2010). Global evaluation of the Collection 5 MODIS dark-target aerosol products over land. *Atmospheric Chemistry and Physics*, 10(21), 10399-10420. https://doi.org/10.5194/acp-10-10399-2010

Lynch, P., Reid, J. S., Westphal, D. L., Zhang, J., Hogan, T. F., Hyer, E. A., et al. (2016). An 11-year global gridded aerosol optical thickness reanalysis (v1.0) for atmospheric and climate sciences. *Geoscientific Model Development,* 9(4), 1489-1522. https://doi.org/10.5194/gmd-9-1489-2016

Ma, P. L., Zhang, K,, Shi, J. J., Matsui, T., & Arking, A. (2012). Direct radiative effect of mineral dust on the development of African easterly waves in late summer, 2003–07. *Journal of Applied Meteorology and Climatology,* 51(12), 2090–2104. https://doi.org/10.1175/JAMC-D-11-0215.1

Miller, R. L., & Tegen, I. (1998). Climate response to soil dust aerosols. *Journal of Climate,* 11(12), 3247–3267. https://doi.org/10.1175/1520-0442(1998)011<3247:CRTSDA>2.0.CO;2

Nathan, T. R., Grogan, D. F. P, & Chen, S. H. (2017). Subcritical destabilization of African easterly waves by Saharan mineral dust. *Journal of the Atmospheric Sciences*, 74(4), 1039–1055. https://doi.org/10.1175/JAS-D-16-0247.1

Nowottnick, E. P., Colarco, P. R., Braun, S. A., Barahona, D. O., da Silva, A., Hlavka, D. L., et al. (2018). Dust impacts on the 2012 Hurricane Nadine track during the NASA HS3 field campaign. *Journal of the Atmospheric Sciences*, 75(7), 2473-2489. https://doi.org/10.1175/JAS-D-17-0237.1

Nowottnick, E., Colarco, P., da Silva, A., Hlavka, D., & McGill, M. (2011). The fate of Saharan dust across the Atlantic and implications for a central American dust barrier. *Atmospheric Chemistry and Physics*, 11(16), 8415-8431. https://doi.org/10.5194/acp-11-8415-2011

O'Neill, N. T., Eck, T. F., Smirnov, A., Holben, B. N., & Thulasiraman, S. (2003). Spectral discrimination of coarse and fine mode optical depth. *Journal of Geophysical Research: Atmospheres*, 108(D17), 4559. https://doi.org/10.1029/2002JD002975

Pan, B., Wang, Y., Hu, J., Lin, Y., Hsieh, J-S., Logan, T. et al., (2018). Impacts of Saharan dust on Atlantic regional climate and implications for tropical cyclones. *Journal of Climate,* 31(18), 7621-744. https://doi.org/10.1175/JCLI-D-16-0776.1

Patricola, C. M., Saravanan, R., & Chang, P. (2014). The impact of the El Niño-Southern Oscillation and Atlantic Meridional Mode on seasonal Atlantic tropical cyclone activity. *Journal of Climate,* 27(14), 5311-5328. https://doi.org/10.1175/JCLI-D-13-00687.1

Pratt, A. S., & Evans, J. L. (2008). Potential impacts of the Saharan Air Layer on numerical model forecasts of North Atlantic tropical cyclogenesis. *Weather and Forecasting*, 24(2), 420-435. https://doi.org/10.1175/2008WAF2007090.1

Prospero, J. M. (1999). Long-term measurements of the transport of African mineral dust to the southeastern United States: Implications for regional air quality. *Journal of Geophysical Research: Atmospheres*, 104(D13), 15917–15927. https://doi.org/10.1029/1999JD900072

Prospero, J. M. (2014). Characterizing the temporal and spatial variability of African dust over the Atlantic. *Past Global Changes Magazine,* 22(2), 68-69. https://doi.org/10.22498/pages.22.2.68

Prospero, J. M., & Lamb, P. J. (2003). African droughts and dust transport to the Caribbean: Climate change implications. *Science,* 302(5647), 1024-1027. https://doi.org/10.1126/science.1089915

Prospero, J. M., & Nees, R. T. (1986). Impact of the North African drought and El Niño on mineral dust in the Barbados trade winds. *Nature,* 320, 735. https://doi.org/10.1038/320735a0

Randles, C. A., daSilva, A. M., Buchard, V., Colarco, P. R., Darmenov, A., Govindaraju, R., et al. (2017). The MERRA-2 aerosol reanalysis, 1980 onward. Part I: System description and data assimilation evaluation. *Journal of Climate,* 30(17), 6823-6850. https://doi.org/10.1175/JCLI-D-16-0609.1

Reale, O., Lau, W. K., Kim, K. M., & Brin, E. (2009). Atlantic tropical cyclogenetic processes during SOP-3 NAMMA in the GEOS-5 global data assimilation and forecast system. *Journal of Atmospheric Sciences,* 66(12), 3563–3578. https://doi.org/10.1175/2009JAS3123.1

Reale, O., Lau, K. M, & da Silva, A. (2011). Impact of interactive aerosol on the African easterly jet in the NASA GEOS-5 global forecasting system. *Weather and Forecasting,* 26(4), 504–519. https://doi.org/10.1175/WAF-D-10-05025.1

Reed, K. A., Bacmeister, J. T., Huff, J. J. A., Wu, X., Bates, S. C., & Rosenbloom, N. A. (2019). Exploring the impact of dust on North Atlantic hurricanes in a high-resolution climate model.Geophysical Research Letters, 46, 1105–1112. https://doi.org/10.1029/2018GL080642

Reid, J. S., Kinney, J. E., Westphal, D. L., Holben, B. N., Welton, E. J., Tsay, S-C., et al. (2003). Analysis of measurements of Saharan dust by airborne and ground-based remote sensing methods during the Puerto Rico Dust Experiment (PRIDE). *Journal of Geophysical Research: Atmospheres,* 108, 8586. https://doi.org/10.1029/2002JD002493

Reynolds, R.W., Rayner, N. A., Smith, T. M., Stokes, D. C., & Wang, W. (2002). An improved in situ and satellite SST analysis for climate. *Journal of Climate,* 15(13)*,* 1609–1625. https://doi.org/10.1175/1520-0442(2002)015<1609:AIISAS>2.0.CO;2

Riemer, N., O. M. Doherty, and S. Hameed (2006), On the variability of African dust transport across the Atlantic, *Geophys. Res. Lett.*, 33, L13814, doi:10.1029/2006GL026163.

Rienecker, M. M., Suarez, M. J., Gelaro, R., Todling, R., Bacmeister, J., Liu, E., et al. (2011). MERRA: NASA's Modern Era Retrospective Analysis for Research and Applications. *Journal of Climate,* 24(14), 3624-3648. https://doi.org/10.1175/JCLI-D-11-00015.1

Rosenfeld, D., Khain, A., Lynn, B., & Woodley, W. L. (2007). Simulation of hurricane response to suppression of warm rain by sub-micron aerosols. *Atmospheric Chemistry and Physics,* 7(13), 3411-3424. https://doi.org/10.5194/acp-7-3411-2007

Sassen, K., DeMott, P. J., Prospero, J. M. & Poellot, M. R. (2003): Saharan dust storms and indirect aerosol effects on clouds: CRYSTAL-FACE results. *Geophysical Research Letters*, 30(12), 1633. https://doi.org/10.1029/2003GL017371

Saunders, M. A., Klotzbach, P. J., & Lea, A. S. (2017). Replicating annual North Atlantic hurricane activity 1878-2012 from environmental variables. *Journal of Geophysical Research: Atmospheres,* 122(12), 6284-6297. https://doi.org/10.1002/2017JD026492

Saunders, M. A., Klotzbach. P. J., Lea, A. S. R., Schreck, C. J., & Bell, M. M. (2020). Quantifying the probability and causes of the surprisingly active 2018 North Atlantic hurricane season. Manuscript submitted to *Earth and Space Science.*

Sessions, W. R., Reid, J. S., Benedetti, A., Colarco, P. R., da Silva, A., Lu, S., Sekiyama, T., Tanaka, T. Y., Baldasano, J. M., Basart, S., Brooks, M. E., Eck, T. F., Iredell, M., Hansen, J. A., Jorba, O. C., Juang, H.-M. H., Lynch, P., Morcrette, J.-J., Moorthi, S., Mulcahy, J., Pradhan, Y., Razinger, M., Sampson, C. B., Wang, J., and Westphal, D. L. (2015). Development towards a global operational aerosol consensus: basic climatological characteristics of the International Cooperative for Aerosol Prediction Multi-Model Ensemble (ICAP-MME), Atmos. Chem. Phys., 15, 335-362.

Sharma, S.S., Kleinbaum, D.G., & Kupper, L.L. (1978). Applied Regression Analysis and Other Multivariate Methods. https://doi.org/10.2307/3150614

Shi, Y., Zhang, J., Reid, J. S., Holben, B., Hyer, E. J., & Curtis, C. (2011). An analysis of the collection 5 MODIS over-ocean aerosol optical depth product for its implication in aerosol assimilation, *Atmospheric Chemistry and Physics,* 11(2), 557-565. https://doi.org/10.5194/acp-11-557-2011

Sippel, J. A., Braun, S. A., & Shie, C.-L. (2011). Environmental influences on the strength of Tropical Storm Debby (2006). *Journal of the Atmospheric Sciences,* 68(11), 2557–2581. https://doi.org/10.1175/2011JAS3648.1

Strong, J. D. O., Vecchi, G. A., &Ginoux, P. (2018). The climatological effect of Saharan dust on global tropical cyclones in a fully coupled GCM. Journal of Geophysical Research:Atmospheres, 123, 5538–5559.https://doi.org/10.1029/2017JD027808

Sobel, Camargo, and Previdi, 2019: Aerosol vs. greenhouse gas effects on tropical cyclone potential intensity and the hydrologic cycle. *Journal of Climate*, doi:10.1175/JCLI-D-18-0357.1

Sun, D., Lau, K. M., & Kafatos, M. (2008). Contrasting the 2007 and 2005 hurricane seasons: Evidence of possible impacts of Saharan dry air and dust on tropical cyclone activity in the Atlantic basin. *Geophysical Research Letters*, 35, L15405. https://doi.org/10.1029/2008GL034529

Tang, B.H., & Neelin, J. D. (2004). ENSO influence on Atlantic hurricanes via tropospheric warming. *Geophysical Research Letters,* 31(24), L24204. https://doi.org/10.1029/2004GL021072

1148   Tompkins A. M., Cardinali, C., Morcrette, J. J., & Rodwell, M. (2005). Influence of aerosol
1149   climatology on forecasts of the African easterly jet. *Geophysical Research Letters,* 32(10),
1150   L10801. https://doi.org/10.1029/2004GL022189
1151   Tsamalis, C., Chedin, A., Pelon, J., & Capelle, V. (2013). The seasonal vertical distribution of
1152   the Saharan Air Layer and its modulation by the wind. *Atmospheric Chemistry and Physics,*
1153   13(22), 11235-11257. https://doi.org/10.5194/acp-13-11235-2013
1154   Towhy, C. H., Kreidenweis, S. M., Eidhammer, T., Browell, E.V., Heymsfield A. J., Bansemer,
1155   A. R., et al. (2009). Saharan dust particles nucleate droplets in eastern Atlantic clouds.
1156   *Geophysical Research Letters*, 36, L01807. https://doi.org/10.1029/2008GL035846
1157   Wang, C., Dong, S., Evan, A. T., Foltz, G. R., & Lee, S. (2012). Multidecadal covariability of
1158   North Atlantic sea surface temperature, African dust, Sahel rainfall and Atlantic hurricanes.
1159   *Journal of Climate,* 25(15), 5404-5415. https://doi.org/10.1175/JCLI-D-11-00413.1
1160   Westphal, D. L., Toon, O. B., and Carlson, T. N. (1987). A two-dimensional numerical
1161   investigation of the dynamics and microphysics of Saharan dust storms, *Journal of Geophysical*
1162   *Research: Atmospheres*, 92, 3027 – 3049. https://doi.org/10.1029/JD092iD03p03027
1163   Wilcox, E. M., Lau, K. M., & Kim, K. M. (2010). A northward shift of the North Atlantic Ocean
1164   intertropical convergence zone in response to summertime Saharan dust outbreaks. *Geophysical*
1165   *Research Letters,* 37(4), L04804. https://doi.org/10.1029/2009GL041774
1166   Xian, P., Reid, J. S., Turk, J. F., Hyer, E. J., & Westphal, D. L. (2009). Impact of modeled versus
1167   satellite measured tropical precipitation on regional smoke optical thickness in an aerosol
1168   transport model. *Geophysical Research Letters*, 36, L16805.
1169   https://doi.org/10.1029/2009GL038823
1170   Xian, P., Reid, J. S., Hyer, E. J., Sampson, C. R., Rubin, J. I., Ades, M., et. al., (2019). Current
1171   State of the global operational aerosol multi-model ensemble: an update from the International
1172   Cooperative for Aerosol Prediction (ICAP). *Quarterly Journal of the Royal Meteorological*
1173   *Society*. Published online Feb 4, 2019. https://doi.org/10.1002/qj.3497
1174   Zhang, H., McFarquhar, G. M., Cotton, W. R., & Deng, Y. (2009). Direct and indirect impacts of
1175   Saharan dust acting as cloud condensation nuclei on tropical cyclone eyewall development.
1176   *Geophysical Research Letters,* 36, L06802. https://doi.org/10.1029/2009GL037276
1177   Zhang, H., McFarquhar, G. M., Saleeby, S. M., & Cotton, W. R. (2007). Impacts of Saharan dust
1178   as CCN on the evolution of an idealized tropical cyclone. *Geophysical Research Letters,* 34,
1179   L14812. https://doi.org/10.1029/2007GL029876
1180   Zhang, J., & Reid, J. S. (2006). MODIS aerosol product analysis for data assimilation:
1181   Assessment of over-ocean level 2 aerosol optical thickness retrievals. *Journal of Geophysical*
1182   *Research: Atmospheres*, 111(D22207). https://doi.org/10.1029/2005JD006898
1183   Zhang, J., J. S. Reid, R. Alfaro-Contreras, and P. Xian (2017), Has China been exporting less
1184   particulate air pollution over the past decade?, Geophys. Res. Lett., 44, 2941–2948, doi:10.1002/
1185   2017GL072617.
1186
1187
1188
1189
1190
1191
1192

Tables:

Table 1. Root mean square error of total AOD (left number in each cell) and coarse-mode AOD (right number in each cell) at 550nm from individual aerosol reanalyses, including CAMSRA, MERRA-2, NAAPS-RA, and the Multi-Reanalysis-Consensus (MRC) verified with AERONET V3L2 monthly data for the 2003-2018 time period. The rank of MRC among all reanalyses in terms of RMSE is also shown. "~" means there are ties in the ranking. The first five sites are located in North Africa or off of the northwestern coast of Africa. The last four sites are located in or near the Caribbean Sea. AOD time series of MRC and AERONET at Dakar, Capo Verde, Ragged Point and La Parguera sites are presented in Figure 3.

Site	CAMSRA	MERRA-2	NAAPS-RA	MRC	Rank of MRC
Banizoumbou	0.13 | 0.17	0.10 | 0.10	0.11 | 0.13	0.10 | 0.11	~1 | 2
Capo Verde	0.07 | 0.07	0.06 | 0.05	0.06 | 0.07	0.06 | 0.06	~1 | 2
Dakar	0.07 | 0.11	0.07 | 0.07	0.08 | 0.10	0.06 | 0.08	1 | 2
La Laguna	0.06 | 0.05	0.06 | 0.05	0.06 | 0.05	0.05 | 0.04	1 | 1
Santa Cruz Tenerife	0.04 | 0.04	0.04 | 0.04	0.04 | 0.04	0.03 | 0.03	1 | 1
Ragged Point	0.05 | 0.03	0.03 | 0.03	0.03 | 0.03	0.04 | 0.03	3 | ~1
La Parguera	0.05 | 0.02	0.03 | 0.02	0.03 | 0.02	0.03 | 0.02	~1 | ~1
Guadeloupe	0.05 | 0.05	0.05 | 0.04	0.04 | 0.05	0.04 | 0.04	~1 | ~1
Key Biscayne	0.05 | 0.03	0.03 | 0.02	0.02 | 0.02	0.03 | 0.02	2 | ~1

1205   **Table 2.** Annual average Atlantic TC activity in the three seasons with the highest JJA

1206   Caribbean DAOD (2014, 2015 and 2018) and the three seasons with the lowest JJA Caribbean

1207   DAOD (2005, 2011 and 2017). Ratios between the three low and the three high DAOD seasons

1208   are also provided. Corresponding numbers for the Caribbean are provided in parentheses next to

1209   the total basin-wide numbers.

	Tropical Depressions and Named Storms	Named Storms	Hurricanes	Major Hurricanes	Accumulated Cyclone Energy
Three highest JJA Caribbean DAOD	12.3 (2.3)	11.3 (2.3)	6.0 (0.3)	2.0 (0.0)	86 (3)
Three lowest JJA Caribbean DAOD	23.0 (6.7)	21.3 (6.7)	10.7 (3.0)	5.7 (2.7)	199 (39)
Ratio	1.9 (2.9)	1.9 (3.0)	1.8 (9.0)	2.8 (N/A)	2.3 (13.0)

1210

1211

1212

Table 3. Correlation matrix between regionally-averaged multi-reanalysis-consensus (MRC) JJA tropical North Atlantic/Caribbean DAOD and 850 hPa U, 200 hPa U, 200 hPa minus 850 hPa U (zonal wind shear), 700 hPa RH, SST, Maximum Potential Intensity (MPI) and Genesis Potential Index (GPI) during JJA and ASO, respectively. Correlations that are statistically significant at the 90% level are highlighted in bold and those with asterisks are statistically significant at the 95% level. 850 hPa relative vorticity is not shown as none of these correlations were statistically significant.

Environmental Field	JJA tropical North Atlantic / JJA Caribbean	ASO tropical North Atlantic / ASO Caribbean
850 hPa U	**-0.63* / -0.79***	0.03 / **-0.66***
200 hPa U	0.34 **/ 0.81***	0.30 / **0.85***
200 minus 850 hPa U	0.43 **/ 0.83***	0.22 / **0.82***
700 hPa RH	-0.43 **/ -0.80***	-0.34 / **-0.55***
SST	**-0.71* / -0.75***	**-0.44** / -0.79*
MPI	**-0.74* / -0.68***	**-0.47** / -0.67*
GPI	**-0.75* / -0.76***	**-0.62* / -0.69***

1223 **Table 4.** Correlation matrix between JJA and ASO values of 850 hPa U, 200 hPa U, 200 minus
1224 850 hPa U, 700 hPa RH and SST over the tropical North Atlantic and the Caribbean,
1225 respectively. Correlations that are statistically significant at the 90% level are highlighted in
1226 bold, and those with asterisks are statistically significant at the 95% level.

Environmental Field	Tropical North Atlantic	Caribbean
850 hPa U	**0.51***	**0.84***
200 hPa U	**0.71***	**0.88***
200 minus 850 hPa U	**0.72***	**0.90***
700 hPa RH	**0.48**	**0.74***
SST	**0.77***	**0.85***

1227

1228

Table 5: Correlations of MRC JJA Caribbean DAOD or JJA tropical North Atlantic (TATL) DAOD with the JJA or ASO Oceanic Nino Index (ONI) and the AMM. Correlations that are statistically significant at the 90% level are highlighted in bold. Correlations that are statistically significant at the 95% level are marked with *.

	JJA Caribbean DAOD				JJA TATL DAOD			
	CAMSRA	MERRA-2	NAAPS-RA	MRC	CAMSRA	MERRA-2	NAAPS-RA	MRC
JJA ONI	0.33	0.29	**0.50**	**0.44**	0.24	0.18	0.28	0.26
ASO ONI	0.42	0.41	**0.61***	**0.54***	0.38	0.30	0.42	0.41
JJA AMM	**-0.72***	**-0.70***	**-0.63***	**-0.76***	**-0.58***	**-0.65***	-0.36	**-0.60***
ASO AMM	-0.42	**-0.45**	-0.30	**-0.45**	-0.33	**-0.52***	0.01	-0.33

Table 6. Partial correlation matrix between MRC JJA Caribbean and tropical North Atlantic (TATL) DAOD and annual Atlantic basin-wide ACE while controlling for ENSO (using the JJA ONI) and the AMM (using JJA AMM index). Linear correlations (without controlling for the climate modes) between DAOD and ACE, AMM and ENSO indices and ACE are also listed for comparison purposes. Correlations that are statistically significant at the 90% level are highlighted in bold, and those with asterisks are statistically significant at the 95% level. Note that the thresholds for statistical significance are different for partial correlation and linear correlation, as the degrees of freedom are different between the two.

	ACE (ctrl. for ENSO)	ACE (ctrl. for AMM)	ACE	ACE (ctrl. for Caribbean DAOD)	ACE (ctrl. for TATL DAOD)
MRC Caribbean DAOD	**-0.62***	-0.29	**-0.61***	-	-
MRC TATL DAOD	-0.39	-0.07	-0.41	-	-
AMM index (JJA/ASO)	-	-	**0.59*/0.45**	0.26/0.26	**0.48**/0.37
ONI (JJA/ASO)	-	-	-0.12/-0.20	0.20/0.18	-0.02/-0.05

1246

1247 **Figures:**

1248
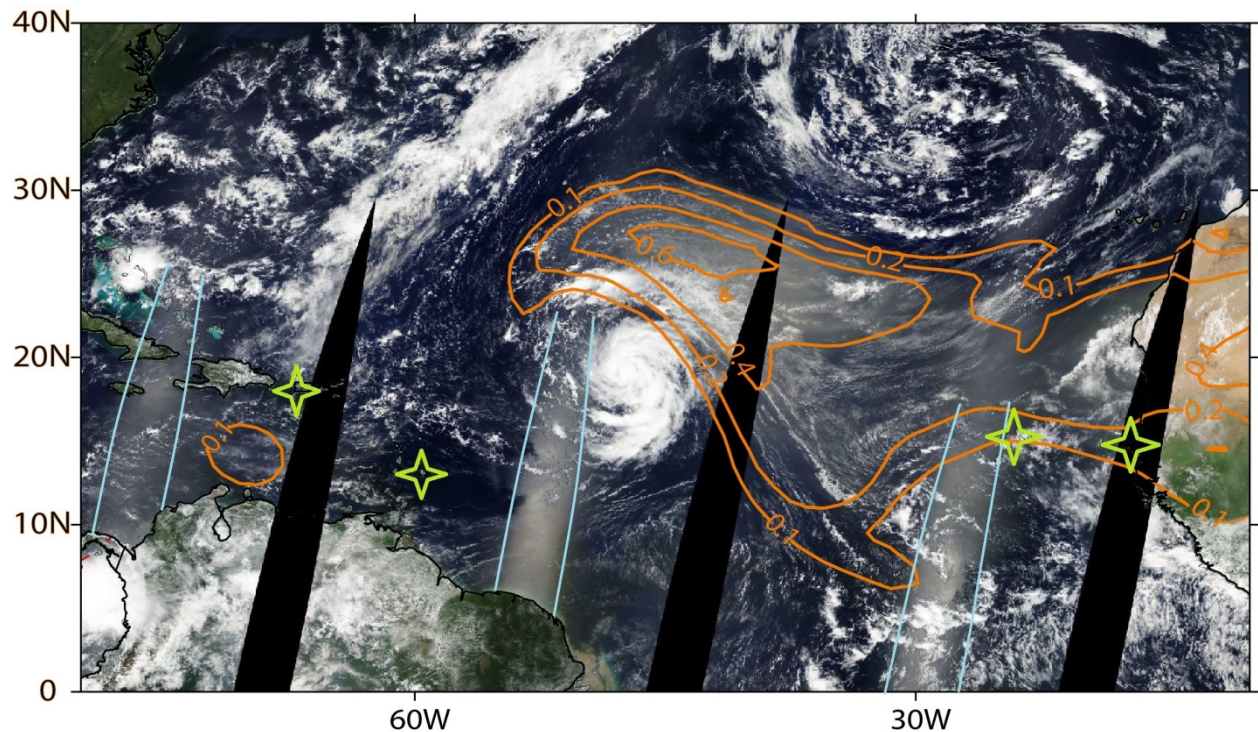
1249 **Figure 1.** True-color Terra MODIS satellite imagery composited on 12 September 2012 and
1250 overlaid with NAAPS-RA 550 nm dust aerosol optical depth (DAOD, an approximate measure
1251 of total atmospheric column of dust aerosol mass, unitless) isopleths, showing Hurricane
1252 Nadine's interaction with the SAL. Nadine is located in the middle of the image. African dust
1253 appears as a light transparent brown haze in between the African coast and Nadine and wrapping
1254 around the northern periphery of the storm. Note that areas of sunglint (narrow regions between
1255 the light blue curves) are similar in color to the dust aerosols, but have the same orientation as
1256 the satellite orbits and are located approximately mid-way between satellite coverage gaps (black
1257 regions oriented south-southwest to north-northeast). Satellite imagery courtesy of the Moderate
1258 Resolution Imaging Spectroradiometer (MODIS) flying on NASA's Terra satellite and available
1259 from https://worldview.earthdata.nasa.gov/. The stars in light green represent four sites used for
1260 validation purposes, including Dakar, Capo Verde, Ragged Point and La Parguera in order from
1261 east to west.

1262

1263

1264
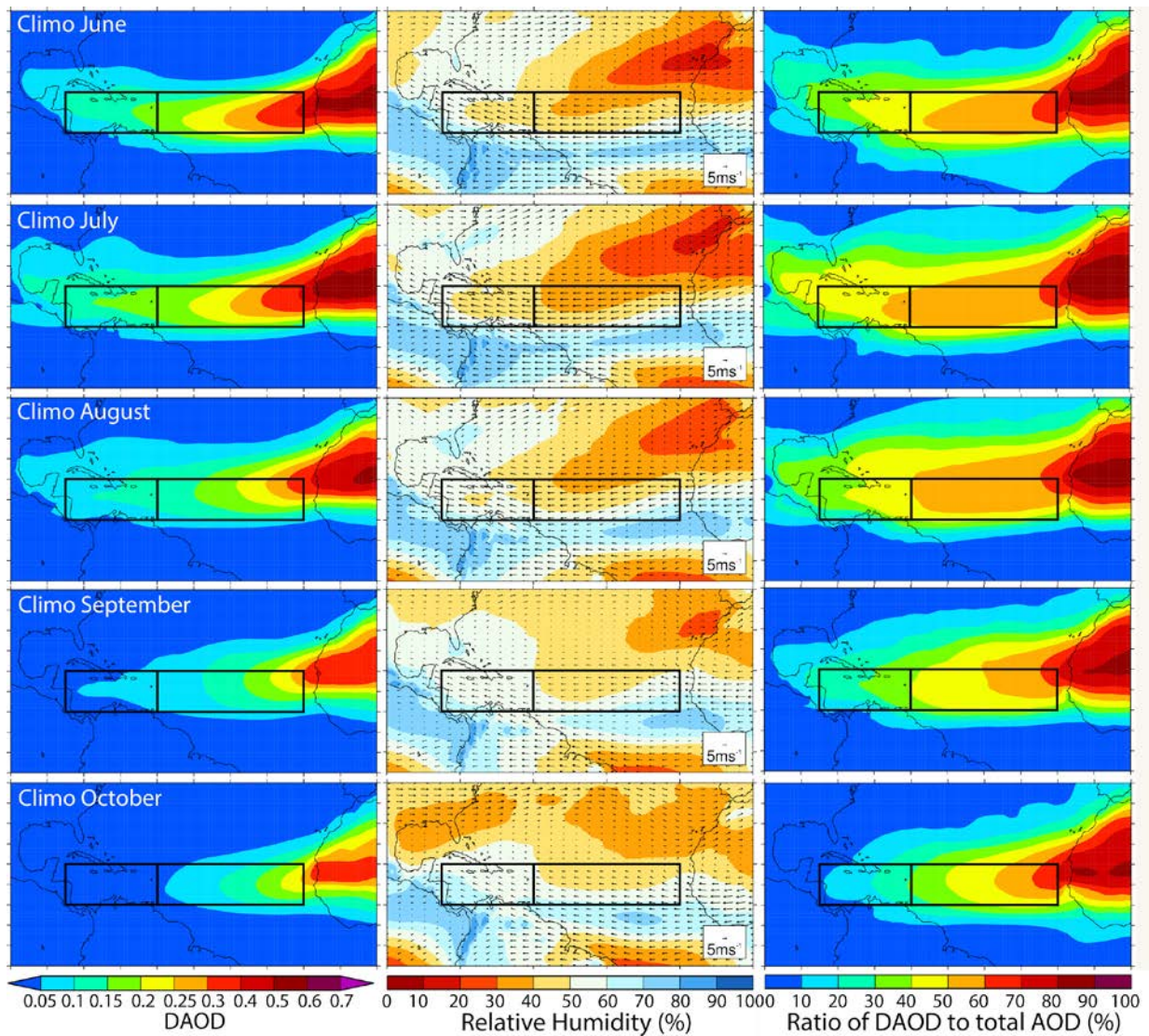
Figure 2. Climatological (2003-2018 average) monthly mean DAOD (left column) and the ratio of DAOD to total AOD (right column) for June-October based on the MRC. The middle column shows the climatological 700 hPa RH (color shading) and horizontal wind vectors from ERA-Interim. Black boxes denote the MDR, including the Caribbean (left, 10º-20ºN, 85º-60ºW) and the tropical North Atlantic (right, 10º-20ºN, 60º-20ºW, denoted "TATL").

1271
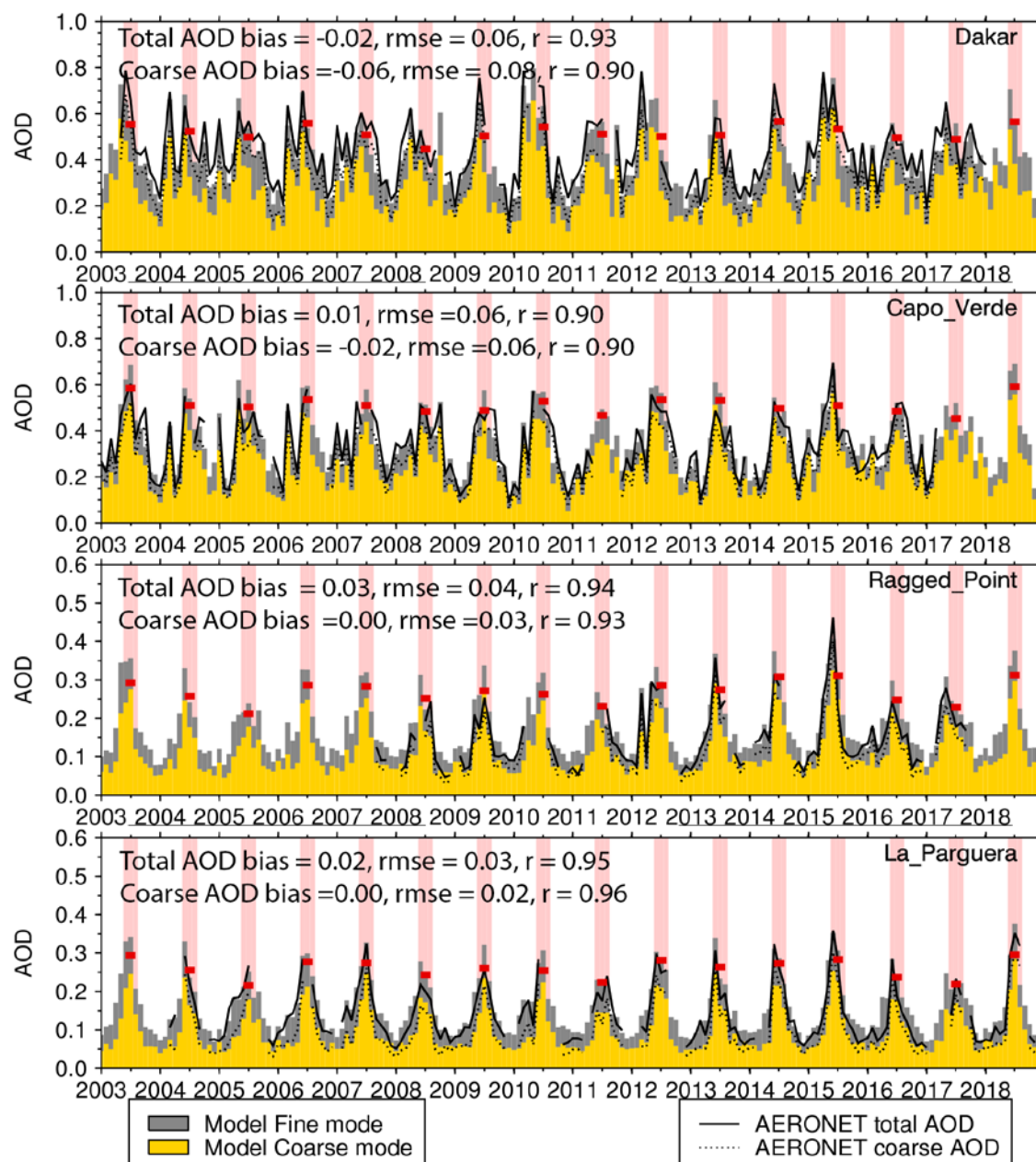
Figure 3. Monthly mean Version 3 L2 AERONET and MRC 550nm modal AODs at four African dust-impacted sites: Dakar, Cape Verde, Ragged Point and La Parguera from east to west. JJA are highlighted with pink shading ,and JJA seasonal average total AOD from MRC are shown with red bars. Annotations for each time series show bias, RMSE and correlation (*r*) of monthly averages calculated from the MRC.
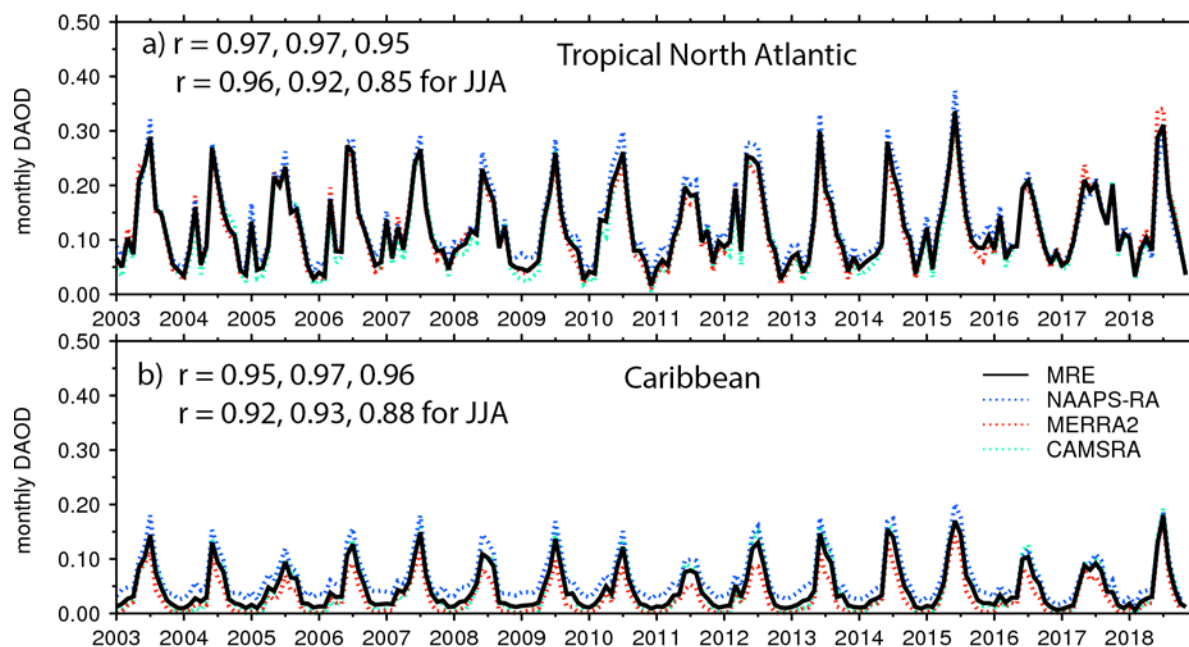
1280
Figure 4. Monthly DAOD at 550nm from CAMSRA, MERRA-2, NAAPS-RA and MRC from
2003-2018 for the (a) tropical North Atlantic and the (b) Caribbean. Correlations between
CAMSRA and MERRA-2, CAMSRA and NAAPS-RA, MERRA-2 and NAAPS-RA are
displayed in sequence for all months and for JJA-only respectively.

1285

1286
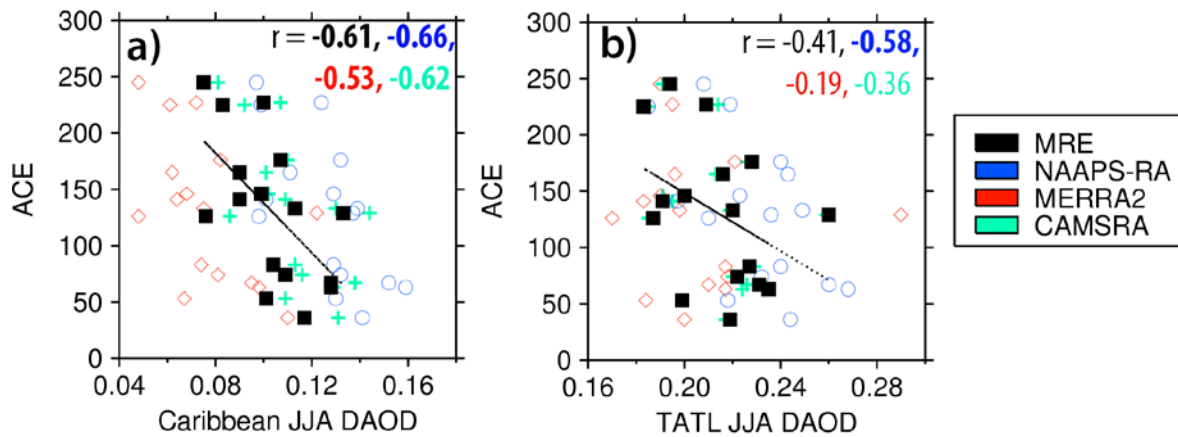
Figure 5. Scatterplot showing the relationship between annual Atlantic Accumulated Cyclone
Energy (ACE) and JJA region-averaged DAOD from MRC, NAAPS-RA, MERRA-2 and
CAMSRA over the (a) Caribbean and (b) the tropical North Atlantic. One unit of ACE equals 10^4
kt^2. Correlations (r) between ACE and DAOD are color-coded for different DAOD products and
overlaid on each plot, and statistically significant correlations are in bold. The possible causes of
the DAOD difference between the reanalysis products are discussed in Section 3.1.

1293

1294
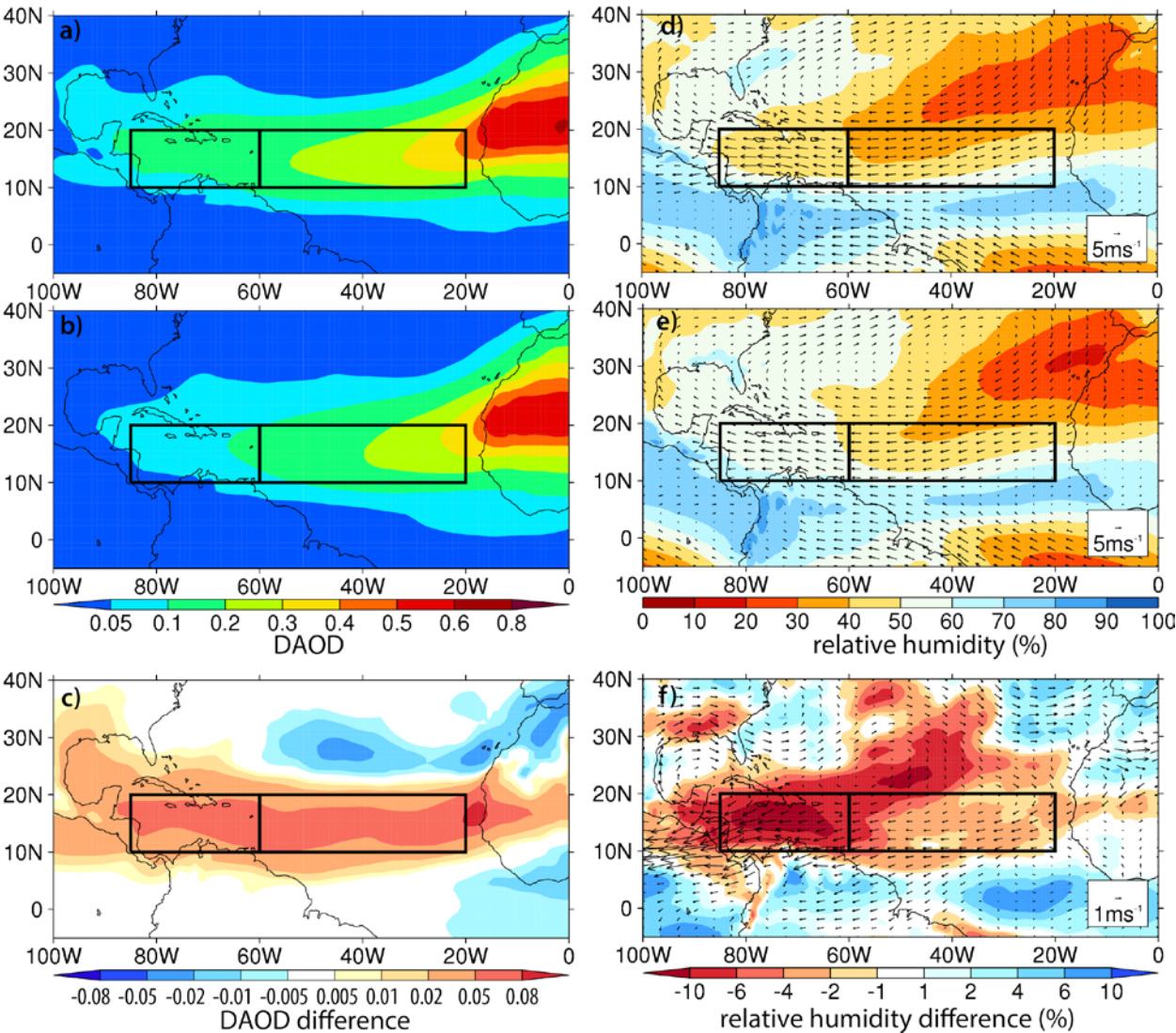
1295
Figure 6. Left: MRC JJA composite of DAOD for the three Atlantic hurricane seasons from
2003-2018 with (a) the highest JJA Caribbean DAOD (2014, 2015 and 2018), (b) the lowest JJA
Caribbean DAOD (2005, 2011, and 2017), and (c) the difference between the two (highest minus
lowest). Right: The corresponding JJA composite of 850 hPa wind (vectors) and 700 hPa RH
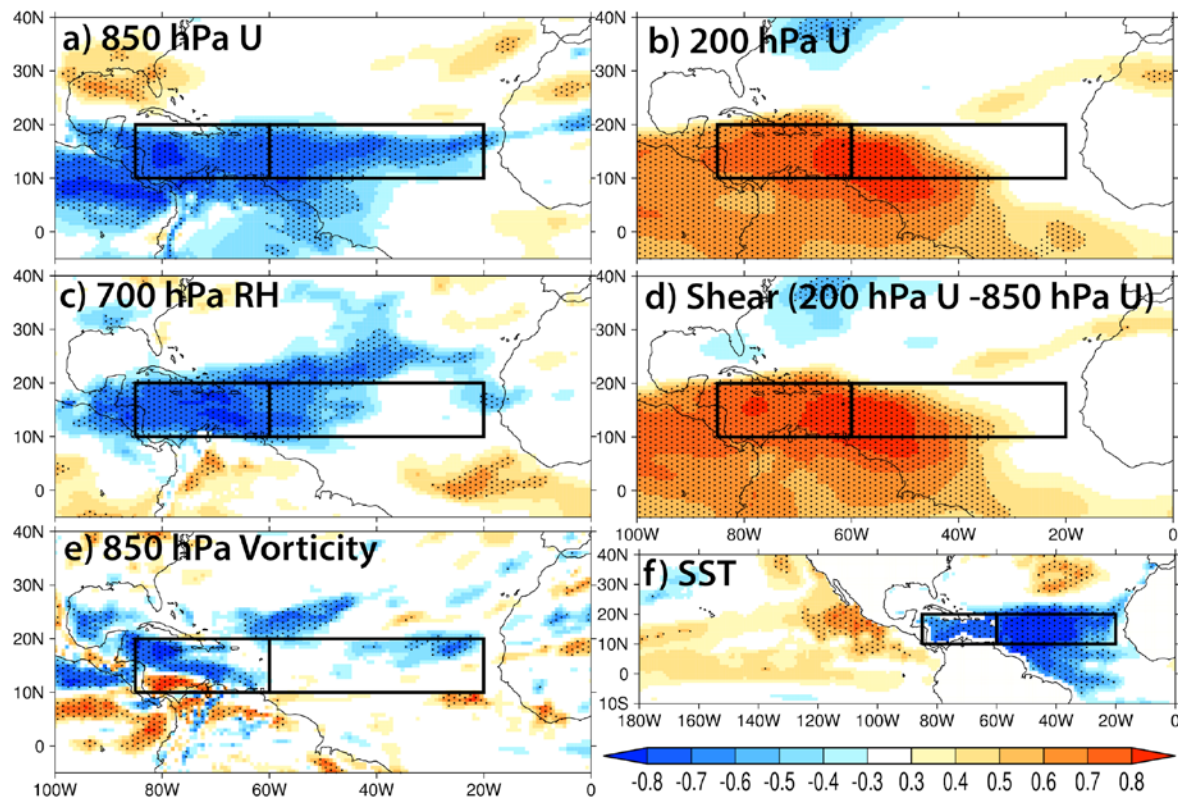(color shading).

1301

1302
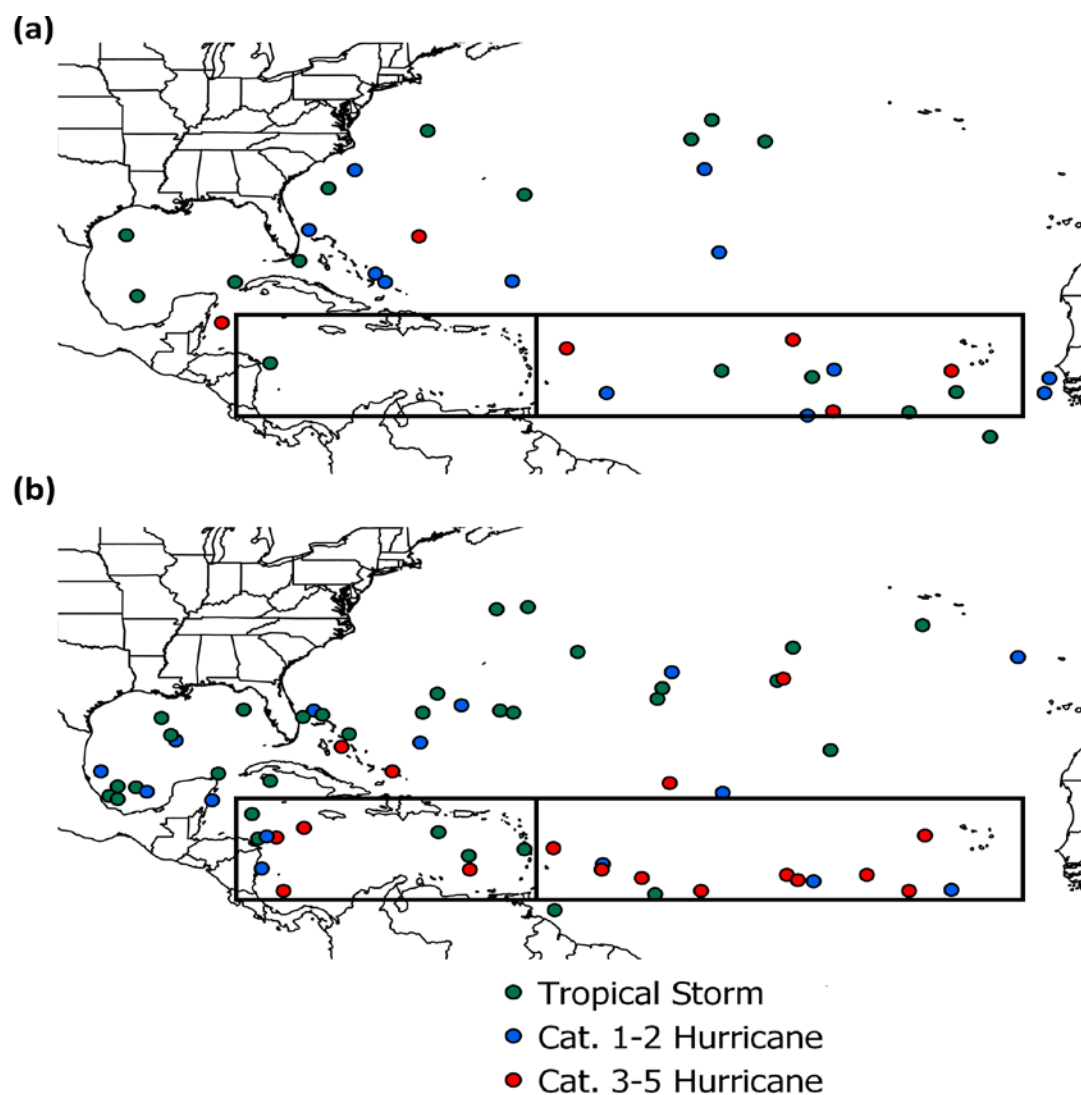
1303

1304

Figure 7. Formation locations of Atlantic named storms during the three seasons with (a) the highest Caribbean JJA DAOD (2014, 2015 and 2018) and (b) the lowest Caribbean JJA DAOD (2005, 2011, and 2017). Also displayed are the maximum intensity that each TC reached.

1308

1309

1310 **Figure 8.** Correlation between MRC JJA regionally-averaged DAOD in the Caribbean and JJA

1311 (a) 850 hPa U, (b) 200 hPa U, (c) 700 hPa RH, (d) zonal wind shear, (e) 850 hPa relative

1312 vorticity and (f) SST. Correlations over the black dotted areas are statistically significant.

1313

1314
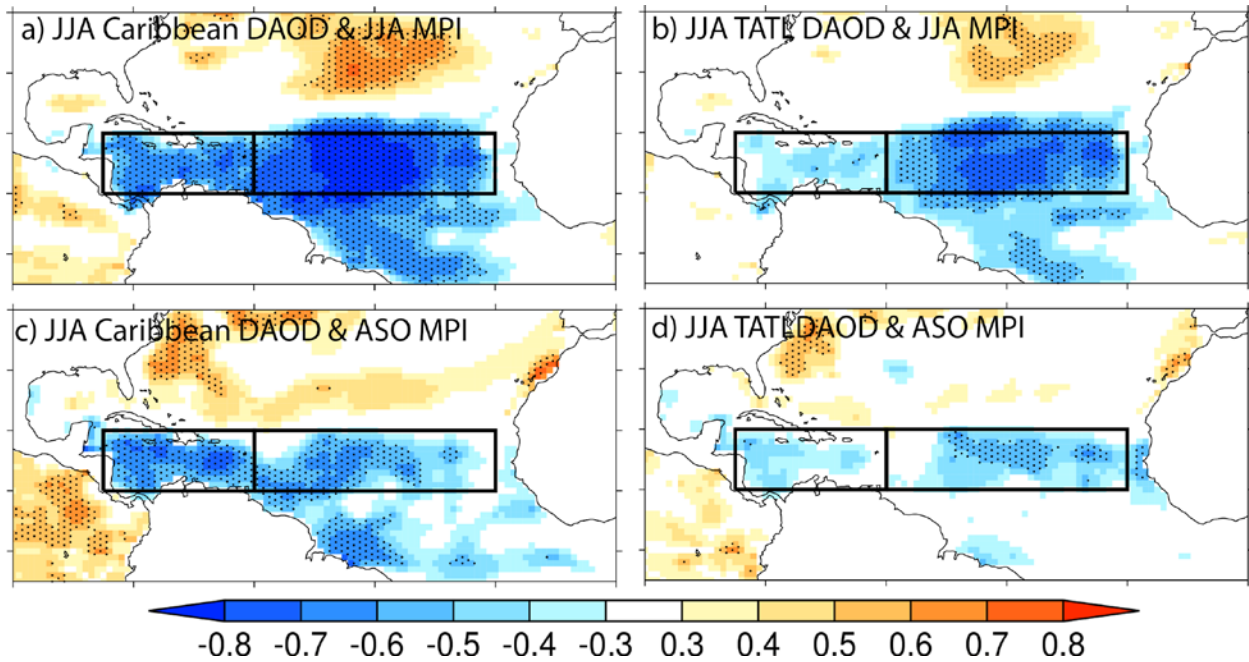
Figure 9. Correlation between (a) MRC JJA regionally-averaged DAOD in the Caribbean and JJA Maximum Potential Intensity (MPI), (b) MRC JJA regionally-averaged DAOD in the tropical North Atlantic (TATL) and JJA MPI, (c) JJA Caribbean DAOD and ASO MPI and (d) JJA TATL DAOD and ASO MPI. Correlations over the black dotted areas are statistically significant.
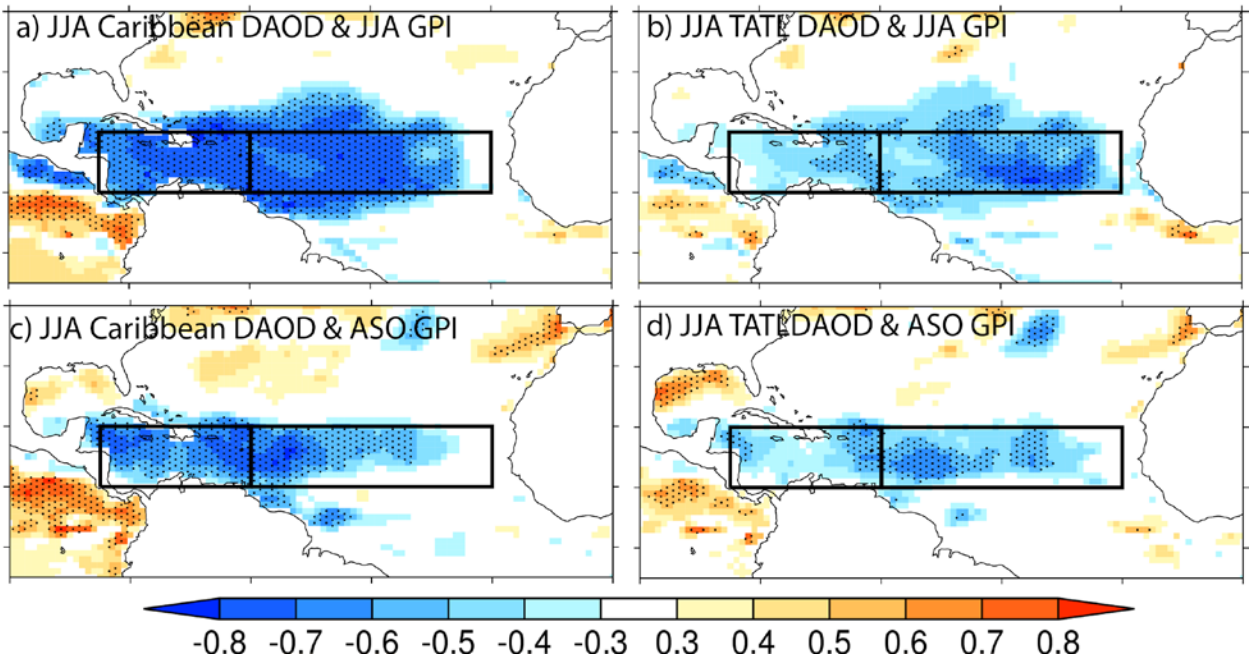
Figure 10. As in Fig. 9, but for the Genesis Potential Index (GPI).